FEDERAL UNIVERSITY OF TECHNOLOGY - PARANÁ
GRADUATE PROGRAM IN ELECTRICAL AND COMPUTER ENGINEERING

ROBERTO WILHELM KRAUSS MARTINEZ

ENERGY EFFICIENCY OPTIMIZATION IN WIRELESS COMMUNICATIONS EMPLOYING MULTIPLE ANTENNAS AND REALISTIC POWER CONSUMPTION MODEL

DOCTORAL THESIS

CURITIBA
2019

ROBERTO WILHELM KRAUSS MARTINEZ

ENERGY EFFICIENCY OPTIMIZATION IN WIRELESS COMMUNICATIONS EMPLOYING MULTIPLE ANTENNAS AND REALISTIC POWER CONSUMPTION MODEL

Doctoral Thesis submitted to the Graduate Program in Electrical and Computer Engineering of the Federal University of Technology - Paraná as partial fulfillment of the requirements for the degree of "Doctor of Science (D.Sc.)" – Concentration area: Telecommunications and Networks.

Advisor: Prof. Glauber Gomes de Oliveira Brante

Co-Advisor: Prof. Guilherme de Santi Peron

CURITIBA
2019

Dados Internacionais de Catalogação na Publicação

Krauss Martinez, Roberto Wilhelm
Energy efficiency optimization in wireless communications employing multiple antennas and realistic power consumption model [recurso eletrônico] / Roberto Wilhelm Krauss Martinez.-- 2019.
1 arquivo eletrônico (55 f.) : PDF ; 894 KB.

Modo de acesso: World Wide Web.
Texto em inglês com resumo em português.
Tese (Doutorado) - Universidade Tecnológica Federal do Paraná Programa de Pós-graduação em Engenharia Elétrica e Informática Industrial. Área de Concentração: Telecomunicações e Redes, Curitiba, 2019.
Bibliografia: f. 50-54.

1. Engenharia elétrica - Teses. 2. Energia - Consumo. 3. Sistemas de comunicação sem fio. 4. Antenas (Eletrônica). 5. Sistemas MIMO - Modelos matemáticos. 6. Gestão de recursos de rádio (Comunicação sem fio). 7. Redes locais sem fio - Consumo de energia. 8. Otimização matemática. 9. Métodos de simulação. I. Brante, Glauber Gomes de Oliveira, orient. II. Peron, Guilherme de Santi, coorient. III. Universidade Tecnológica Federal do Paraná. Programa de Pós-graduação em Engenharia Elétrica e Informática Industrial. IV. Título.
.

CDD: Ed. 23 -- 621.3

Biblioteca Central do Câmpus Curitiba - UTFPR
Bibliotecária: Luiza Aquemi Matsumoto CRB-9/794

Ministério da Educação
Universidade Tecnológica Federal do Paraná
Diretoria de Pesquisa e Pós-Graduação

TERMO DE APROVAÇÃO DE TESE Nº 201

A Tese de Doutorado intitulada **"Energy efficiency optmization in wireless communications employing multiple antenas and realistic power consumption model",** defendida em sessão pública pelo(a) candidato(a) **Roberto Wilhelm Krauss Martinez**, no dia **27 de setembro de 2019**, foi julgada para a obtenção do título de Doutor em Ciências, **área de concentração Telecomunicações e Redes**, e aprovada em sua forma final, pelo Programa de Pós-Graduação em Engenharia Elétrica e Informática Industrial.

BANCA EXAMINADORA:

Prof(a) Dr(a). Glauber Gomes de Oliveira Brante - Presidente – (UTFPR)
Prof(a) Dr(a). Richard Demo Souza – (UFSC)
Prof(a) Dr(a). Marcelo Eduardo Pellenz – (PUC-PR)
Prof(a) Dr(a). André Augusto Mariano – (UFPR)
Prof(a) Dr(a). João Luiz Rebelatto – (UTFPR)

A via original deste documento encontra-se arquivada na Secretaria do Programa, contendo a assinatura da Coordenação após a entrega da versão corrigida do trabalho.

Curitiba, 27 de setembro de 2019.

ACKNOWLEDGEMENTS

First of all, I would like express my gratitude to GOD, for his grace and for giving me the strength to finish this work.

My sincere appreciation to Professor Glauber Brante for his support, guidance and friendship. Professor Glauber is a really example of life to be follow. Also many thanks to my co-advisor Professor Guilherme Peron for his friendship, guidance, dedication, and for other things like the discussions about history of south America. To Professor Richard Souza, my gratitude, who is always present, for his great advices.

I would like also to express my thanks to all who directly or indirectly contributed to this work, in particular to my mother Mary Stella Martinez de Krauss who was my support in good and bad situations, also to my brother Christopher, to my second family Campos-Januário, who helped me a lot during my doctorate degree.

To all the members of the LabSC, particularly to professors Moritz, Ohara, Marcos, Eduardo Hodgson, and all the students Vinicius, Giovanna, Rafaela Scaciota, Rafaela Schroeder, Fabio, Lucas, etc. for their fellowship and for the great moments.

Also, I would like to thanks to the UTFPR and CPGEI for the opportunity to participate in this program; to CAPES, CNPq and Fundação Araucária for the financial support.

Finally, to all my great friends that I do not name them because they are several, for their friendship and company.

O primeiro passo sempre é querer.

RESUMO

Krauss, R. ENERGY EFFICIENCY OPTIMIZATION IN WIRELESS COMMUNICATIONS EMPLOYING MULTIPLE ANTENNAS AND REALISTIC POWER CONSUMPTION MODEL. 62 f. Doctoral Thesis – Graduate Program in Electrical and Computer Engineering, Federal University of Technology - Paraná. Curitiba, 2019.

Neste trabalho, nos concentramos na eficiência energética em redes de comunicação sem fio, especialmente comparando as vantagens da técnica de seleção de antenas (AS, *Antenna selection*) com outras técnicas de múltiplas entradas e múltiplas saídas (MIMO, *Multiple-input multiple-output*). Portanto, discutimos dois cenários modernos de rede: primeiro consideraramos a implantação estações rádio base de pequeno porte (SBS, *Small base stations*) e, em seguida, uma implantação de rede de dispositivo-a-dispositivo (D2D, *Device-to-device*). No cenário de SBS, analisamos a eficiência energética por área (AEE, *Area energy efficiency*) para as técnicas de seleção de antenas (AS), máxima razão na transmissão (MRT, *Maximal ratio transmission*) e multiplexação espacial (SM, *Spatial multiplexing*). Também empregamos diferentes níveis de atenuação de interferência e um modelo realista de consumo de energia. A partir desse cenário apresentamos a representação matemática e nossos resultados mostram que o AS tem maior AEE que as outras técnicas quando a demanda por capacidade do sistema é baixa, enquanto o SM se torna mais eficiente energeticamente quando a capacidade demandada é maior. No entanto, observamos que o AS tem mais eficiência energética por área para distâncias curtas, isso se deve à menor energia consumida pela cadeia de RF (RF, *Radio Frequency*) em todos os nós. Ainda, podemos concluir que o desempenho do sistema com pequenas SBS, em termos de AEE, é fortemente dependente da quantidade de interferência, que ao mesmo tempo depende do modelo de consumo de energia. Ademais, no cenário de comunicação D2D examinamos a técnica AS em comparação com a técnica MRT. Além disso, também assumimos que os nós D2D estão distribuídos de acordo com um processo de Poisson homogêneo (PPP, *Poisson point process*), os quais interferem uns com os outros. Em outras palavras, eles compartilham o mesmo espectro e empregam um número limitado de bits de *feedback*. Assim, os resultados numéricos mostram que a técnica de MRT possui maior eficiência espectral que o AS para um mesmo número de nós interferentes em uma determinada área. Por outro lado, a distância do par D2D tem um impacto maior no aumento da eficiência energética da área para a rede. Além disso, para curtas distâncias o esquema AS tem melhor desempenho em comparação ao MRT, mesmo quando esse último emprega um número maior de bits de *feedback*. É notavel o melhor desempenho do AS em comparação ao MRT para distâncias curtas quando o número de antenas de transmissão aumenta, ou seja, apesar de proporcionar maior taxa de dados, o aumento do número de antenas no MRT não compromete consideravelmente sua eficiência energética.

Palavras-chave: Técnicas de múltiplas antenas, modelo de consumo de energia, estações rádio base de pequeno porte, comunicação dispositivo-a-dispositivo

ABSTRACT

Krauss, R. ENERGY EFFICIENCY OPTIMIZATION IN WIRELESS COMMUNICATIONS EMPLOYING MULTIPLE ANTENNAS AND REALISTIC POWER CONSUMPTION MODEL. 62 f. Doctoral Thesis – Graduate Program in Electrical and Computer Engineering, Federal University of Technology - Paraná. Curitiba, 2019.

In this work we focus on the energy efficiency in wireless communication networks, especially comparing the advantages of the antenna selection (AS) technique among other multiple-input multiple-output (MIMO) techniques. Therefore, we discuss two different network scenarios: first considering a small base stations (SBS) deployment, and then a device-to-device (D2D) network deployment. In the small SBS scenario we analyze the area energy efficiency (AEE) for antenna selection (AS), maximal ratio transmission (MRT) and spatial multiplexing (SM) techniques. We also employ different interference cancellation levels and a realistic power consumption model. We derive the mathematical representation and our results show that AS has a larger AEE among the other techniques when the demand for system capacity is low, while SM becomes more energy efficient when the demanded capacity is larger. However we observe that AS has more AEE for short distances, which is due to the lower energy consumed by the Radio Frequency (RF) chains in every node. Yet, we can conclude that the system performance with small SBS, in terms of AEE, is strongly dependent on the amount of interference, which at the same time depends on the power consumption model. In addition, our second scenario is the D2D communication network, where we examine the AS technique in comparison with MRT. Furthermore, we also assume that the D2D nodes are distributed according to a homogeneous Poisson process (PPP), which interfere with each other, i.e., share the same spectrum, and they employ a limited number of feedback bits. Therefore, in the numerical result we also observe MRT technique is more spectral efficient than AS regardless of the number of interfering nodes in the area. On the other hand, the distance of the D2D pair has a larger impact in increasing the AEE of the network, with AS outperforming MRT even when the latter employs a larger number of feedback bits. It is also noteworthy the performance of AS in comparison to MRT for short distances when the number of transmit antennas increases, i.e., despite providing higher data rate, measured in terms of the spectral efficiency, the increased number of antennas for MRT does not considerably compromises its energy efficiency.

Keywords: Multiple antennas, power consumption model, small base stations, device-to-device communication

LIST OF FIGURES

Figure 1 – D2D communication 3GPP release 12 standard is based on proximity service, (1) Black - D2D link in-coverage, (2) Blue link out-of-coverage, (3) Violet - partial-covered. 18

Figure 2 – System model of a cellular network composed by N_{BS} hexagonal cells of radius R, covering an area A. 25

Figure 3 – Backhauling Layout. The Radio Remote Units (RRUs) are connect via wireless channel to the Baseband Units (BBUs). Then, the optical backhaul consists of 1 Gbps SFPs (Small Form-Factor Pluggable) connected to the access switch, by its turn connected through a 10 Gbps interface to the border router. 27

Figure 4 – Area power consumption (Ω) as a function of the area throughput (τ_{sch}), varying N_{BS}, with $m_{\mathrm{t}} = m_{\mathrm{r}} = 2$. 31

Figure 5 – Number of SBSs (N_{BS}) as a function of the area throughput (τ), with $m_{\mathrm{t}} = m_{\mathrm{r}} = 2$ and $\kappa = 0$. 31

Figure 6 – Area energy efficiency (η) as a function of the area throughput (τ) for SBSs with $m_{\mathrm{t}} = m_{\mathrm{r}} = 2$ and $\kappa = 0$. The arrow "$\leftarrow \bullet$" indicates the N_{BS} employed by SM, "$\leftarrow \times$" the N_{BS} employed by AS and "$\leftarrow$ o" the N_{BS} employed by MRT. 33

Figure 7 – Area energy efficiency (η) as a function of τ_{sch} for SBSs with $m_{\mathrm{t}} = m_{\mathrm{r}} = 2$ and $\kappa = \{0.1, 1\}$. 34

Figure 8 – Area energy efficiency (η) as a function of the area throughput (τ) for SBSs with $m_{\mathrm{t}} = m_{\mathrm{r}} = 2$ and $\kappa = 0$. 35

Figure 9 – Area energy efficiency (η) as a function of the number of antennas ($m_t = m_r$) with $\kappa = 0$, and with a capacity target of 10 Gbits/s and $N_{\mathrm{BS}} = 10$ for SM technique, $N_{\mathrm{BS}} = 21$ for AS and MRT techniques. 36

Figure 10 – Area energy efficiency (η) as a function of the number of antennas ($m_t = m_r$) with $\kappa = 1$, and with a capacity target of 1 Gbits/s and $N_{\mathrm{BS}} = 117$ for SM technique, $N_{\mathrm{BS}} = 183$ for AS and MRT techniques. 37

Figure 11 – Area power consumption (Ω) as a function of the area throughput (τ), for different antenna configurations with $\kappa = 1$. 37

Figure 12 – Area energy efficiency (η) as a function of κ for $m_t = m_r = 2$, and with a capacity target of 7 Gbits/s. 38

Figure 13 – Area energy efficiency (η) as a function of the coverage area with $\kappa = 0.1$ and $N_{\mathrm{BS}} = 80$. 39

Figure 14 – Area energy efficiency (η) as a function of the coverage area with $\kappa = 1$ and $N_{\mathrm{BS}} = 80$. 39

Figure 15 – D2D communication network with devices located within an area A following a PPP distribution. The index i denotes each D2D link, between Tx_i and Rx_i, whose channel matrix is represented by $\mathbf{H}_i \in \mathbb{C}^{N \times N}$. Moreover, the main link is denoted by $i = 1$ and the interference channels due to neighbor devices communicating at the same time are represented

by $\mathbf{G}_i \in \mathbb{C}^{N \times N}$. 43
Figure 16 – Area sum spectral efficiency (ξ) as a function of the average number of nodes in a fixed area A. The typical distance is $d_1 = 50$ m, $\overline{\gamma} = 60$ dB and $N \in \{2, 4\}$ antennas. 49
Figure 17 – Area energy efficiency (η) vs. SNR ($\overline{\gamma}$), with $N = 2$ and $B = \{1, \infty\}$. .. 49
Figure 18 – Area energy efficiency η as a function of the number of antennas, with $\overline{\gamma}$= 60 [dB]. 51
Figure 19 – Integration of both D2D and SBS networks. 53
Figure 20 – MIMO-OFDM antenna selection: (a)Per-subcarrier,(b)Bulk. 54
Figure 21 – MIMO-OFDM antenna selection extension for Bulk and Per-subcarrier. 55

LIST OF TABLES

Table 1 – System Parameters for Small Base Station Network. 30
Table 2 – System Parameters for the D2D network. 48
Table 3 – Transmit distance up to which AS outperforms MRT in terms of area energy efficiency, for different $\overline{\gamma}$. 50

LIST OF ABBREVIATIONS

EE	Energy Efficiency
BS	Base station
MIMO	Multiple-input/Multiple-output
RF	Radio frequency
AS	Antenna selection
SBS	Small base stations
D2D	Device-to-device
LTE	Long-term evolution
MRT	Maximum ratio transmission
SM	Spatial multiplexing
AEE	Area energy efficiency
PCM	Power consumption model
CSI	Channel state information
MTC	Machine-type communication
PPP	Poisson point process
QoS	Quality of Service
ICIC	Inter-cell interference coordination
CoMP	Coordinated multi-point transmit and reception
SNR	Signal to noise ratio
SIR	Signal-to-interference power ratio
SINR	Signal-to-interference-plus-noise ratio
MRC	Maximum ratio combining
i.i.d.	Independent and identically distributed
PDF	Probability density function
AWGN	Additive white Gaussian noise
CDI	Channel direction information
CDF	Cumulative distribution function

LIST OF NOTATIONS

Small base station network

R	Cell radius
A	Covered Area
N_{BS}	Number of required SBSs
P_{tx}	SBS transmit power
$\mathbf{H}$	Channel gain matrix
$h_{i,j}$	Channel fading coefficients
m_{t}	Number of transmit antennas
$\widehat{m}_{\mathrm{t}}$	Number of *active* transmit antennas
m_{r}	Number of receiving antennas
$\mathbf{x}$	Unit energy transmitted symbol vector
$\mathbf{y}$	Received symbol vector
$\mathbf{w}$	Zero-mean additive white Gaussian noise
N_0	Thermal noise
P_{L}	Path-loss
α	Path loss exponent
d	Transmission distance from the SBS to the UE
G	Antenna gain
L	Link margin
λ	Wavelength
$\overline{\gamma}$	Average SNR
W	Channel bandwidth
κ	Interference factor
P_{I}	Maximum interference power
ζ	Signal-to-interference power ratio
ϵ_{sch}	Signal-to-interference-plus-noise ratio for each sch scheme
sch	MIMO transmission scheme such that sch $\in SM, MRT, AS$
P_{net}	Network total power consumption
ψ	Power amplifier drain efficiency
P_1	Circuitry power consumption
P_2	Power consumption that does not depend on $\widehat{m}_{\mathrm{t}}$
P_{bh}	Power consumption of the backhaul
P_{dl}	Power consumed by the downlink interfaces
P_{ul}	Power consumed by the uplink interfaces
P_{s}	Power consumed by the access switch
$\max_{\mathrm{dl}}$	Maximum number of downlink interfaces available in an aggregation switch
N_{ul}	Number of uplink interfaces
Ag_{tot}	Total traffic aggregated at all switches
$U_{\max}$	Maximum rate supported by each uplink interface
δ	Weighting parameter of the maximum power consumed by the switch

$P_{\text{s,max}}$	Maximum power consumed by the switch
Ag_{switch}	Traffic traversing the switch
Ag_{max}	Maximum traffic supported by the switch
Ω	Area power consumption
τ_{sch}	Area throughput target
$C_{\text{net}}^{(\text{sch})}$	Total network capacity for the sch scheme
η_{sch}	Area energy efficiency of each employed MIMO scheme
$\overline{\gamma}_{\text{sch}}$	Average SNR per receive antenna for sch scheme
$\mathbf{I}_m$	$m \times m$ identity matrix
$\mathbf{H}^{\dagger}$	Conjugate transpose of $\mathbf{H}$
γ_{sch}	Instantaneous SNR for the sch scheme
λ_{max}	Maximum eigenvalue of $\mathbf{\Xi}$

D2D network

ρ	Poisson point process density
N	Number of transmit/receive antennas
d_i	Transmitters distance from a typical receiver
$\mathbf{G}_i$	Interference Matrix channel
$\mathcal{R}_{\text{sch}}$	Spectral efficiency of each employed MIMO scheme
η_{sch}	Area energy efficiency of each employed MIMO scheme
$\mathcal{P}_{\text{sch}}$	Power consumed to transmit one bit of information of each employed MIMO scheme
sch	MIMO transmission scheme such that sch $\in \{\text{MRT}, \text{AS}\}$
P_{t}	Transmission power of D2D user equipment
ψ	Drain efficiency of the power amplifier
$\hat{N}$	Number of *active* antennas at each side, in the D2D network
P_{ctx}	Power consumed by the RF circuitry at the transmitter side in a D2D equipment
P_{crx}	Power consumed by the RF circuitry at the receiver side in a D2D equipment
Rx_1	D2D main link receiver
Tx_i	i-th D2D transmitter
Rx_i	i-th D2D receiver
g_i	Interference channel of the neighbor node
w_1	Additive white Gaussian noise
σ^2	Variance of the additive white Gaussian noise
f	Carrier frequency
c	Speed of light in vacuum
B_{sch}	Number of feedback bits in the sch scheme
$\mathcal{R}_{\text{sch}}$	Spectral efficiency of the sch scheme
$\mathbf{v}_1$	Beamforming vector used at the transmitter
$\mathbf{z}_1$	Combining vector employed at the receiver
$\mathcal{C}$	Beamforming codebook employed for channel state information feedback
B	Number of bits employed in the quantization of the channel direction information

CONTENTS

1 INTRODUCTION **15**
1.1 ENERGY EFFICIENCY WITH SMALL BASE STATIONS 16
1.2 ENERGY EFFICIENCY IN A D2D NETWORK 17
1.3 GOALS 19
1.3.1 General Goal 19
1.3.2 Specific Goals 19
2 ENERGY EFFICIENCY OF MULTIPLE ANTENNA CELLULAR NETWORKS IN BASE STATIONS **21**
2.1 SYSTEM MODEL 24
2.1.1 Network Total Power 26
2.1.2 Area Energy Efficiency 28
2.2 MIMO TRANSMISSION SCHEMES 28
2.2.1 Spatial Multiplexing (SM) 28
2.2.2 Maximal Ratio Transmission (MRT) 29
2.2.3 Antenna Selection (AS) 29
2.3 NUMERICAL RESULTS AND DISCUSSION 30
2.3.1 Area Power Consumption 30
2.3.2 Area Energy Efficiency 32
2.3.3 Different Power Consumption Models 33
2.3.4 Fixed Network Capacity and Area Energy Efficiency 34
2.3.5 Area Energy Efficiency for Different Coverage Areas 36
2.4 CONCLUSIONS 38
3 AREA ENERGY EFFICIENCY IN LIMITED FEEDBACK DEVICE-TO-DEVICE NETWORKS **41**
3.1 SYSTEM MODEL 42
3.2 MIMO TRANSMISSION SCHEMES 43
3.2.1 Antenna Selection (AS) 43
3.2.2 Maximal Ratio Transmission (MRT) 46
3.3 NUMERICAL RESULTS AND DISCUSSION 48
3.4 CONCLUSIONS 50
4 FINAL COMMENTS AND FUTURE EXTENSIONS **52**
BIBLIOGRAPHY **56**
Appendix A – PROOF OF EQUATION (43) **62**

1 INTRODUCTION

The growth in data traffic it is forecast to reach 77 exabytes by 2022, an annual traffic growth of almost one exabytes per year in the next three years, so that the global data traffic is expected to increase seven-fold between 2017 and 2022 according to the constant evaluations of Cisco (CISCO, 2019). This growth, which is in constant demand for more traffic, is also linked to energy consumption since more energy will be required to reach a certain capacity, which in turn is linked to the system's rate. Meanwhile, a key challenge of wireless communication is to find the best spectral efficiency and energy efficiency, which is a compelling compromise.

Truly, enhancing energy efficiency (EE) in wireless networks delivers benefits of reducing global warming (AUER et al., 2011a). Such reduction comes from increasing battery durability in equipment and decreasing the consumption of energy in base stations (BSs) (ASADI et al., 2014). Therefore, Multiple-input Multiple-output (MIMO) techniques are employed to achieve better energy efficiency (FENG et al., 2013), as they are promising techniques for today wireless communications and beyond. Specifically, MIMO techniques have the ability to provide high data rates without consuming a large amount of resources in terms of spectrum and transmit power (RENZO et al., 2014; LIU et al., 2012). In contrast, these techniques exhibit high power consumption by considering that multiple RF chains are used for data transmission.

Among the many available MIMO schemes, antenna selection (AS) is a promising technique to meet the growing demands of energy efficiency (LI et al., 2014). In this technique, there is a hardware reduction since only one RF chain is selected and remains active during transmission (LI et al., 2014), providing: either diversity or multiplexing gains with lower energy consumption (MEHTA et al., 2012).

This work explores antenna selection techniques in two modern wireless network scenarios. First, it is considered a scenario with small base stations (SBSs), where the energy consumption model of the SBSs is fundamental. Specifically, in the employed power consumption model we highlight the energy consumption per RF chain and the backhaul power consumption. Thus, AS is a candidate technique for improving energy efficiency, which is compared to maximal ratio transmission (MRT) and spatial multiplexing SM techniques. Therefore, although MRT and SM are able to prove higher spectral efficiency due to the diversity and multiplexing gains of using multiple antennas, AS has increased energy efficiency, due to a lower power consumption at the circuit level. Next, a D2D

scenario is analyzed, where the interference of neighboring nodes communicating at the same time is a performance limiting factor. Here we compare AS with MRT when the receiver also has multiple antennas. Next, we summarize these two scenarios with more details in the next two sections, where in section 1.1 we introduce the SBS network scenario and in section 1.2 the D2D network scenario.

1.1 ENERGY EFFICIENCY WITH SMALL BASE STATIONS

The data rate growing demand usually requires the deployment of more base stations (BSs) to provide communications in large-scale, which in turn may significantly increase the network power consumption. Since the natural resources used for energy generation are limited and in many cases, non-renewable, there is a global concern about energy efficiency (AUER et al., 2011a). So, while developing the network plan, maximizing the energy efficiency is one of the main targets.

A higher energy efficiency can be achieved by finding the optimal number of BSs to deliver a desired quality of service. Looking forward to improving spectral efficiency, the long-term evolution (LTE) cellular network 4G standard (LIU et al., 2012) employs MIMO technologies aiming to mitigate the effects of fading at the wireless channel, by providing diversity gains through maximum ratio transmission (MRT) techniques, or to increase the network capacity, by providing multiplexing gains through spatial multiplexing (SM) schemes. However, these techniques also lead to a greater energy consumption as a result of the multiple radio frequency (RF) chains, specially due to the power amplifier consumption that corresponds to 55-60% of the total consumption in a BS (AUER et al., 2011a). By choosing a proper MIMO technique, it has been shown that different goals can be achieved, *e.g.*, meeting the increased traffic demand, or reducing the power consumption (RAYEL et al., 2014).

In scenarios where the demanded traffic is not critical, a deployment focused on energy efficiency can rely on AS technique. It is worth noting that LTE already employs AS, but at the user equipment (UE) only (MEHTA et al., 2012), since LTE was first designed to increase the throughput only, not the energy efficiency. In such scenarios, if AS is employed at the BS side, a greater energy efficiency could be achieved, with the same diversity order as in MRT (MOLISCH, 2003), which could also lead to greater area energy efficiency (AEE). Moreover, according to (RAYEL et al., 2014), when analyzed through a realistic power consumption (PCM) model, AS is more energy efficient when compared to SM in the low to medium spectral efficiency region. However, since only

one transmit antenna is selected, the transmit power needed to meet a required spectral efficiency increases at a greater rate for AS when compared to SM, so that in the high spectral efficiency region SM becomes the best choice.

In chapter 2, we analyze the energy efficiency of a cellular network employing MIMO techniques as AS, MRT and SM. In this scenario, the user equipment is subjected to interference from other BSs from the neighboring cells. Moreover, the interference may not be fully canceled due the interference mitigation technique or due imperfect estimation of channel state information (CSI). In addition, for our analysis we employ a realistic PCM that combines the models in (TOMBAZ et al., 2011) and (RAYEL et al., 2014). Consequently, our main contribution shows that AS delivers the largest area energy efficiency among the other MIMO techniques, when the demand for system capacity is low and the inter-cell interference is not fully canceled.

Contributions associated with this chapter can be found in (Krauss et al., 2017) and in (Krauss et al., 2019).

1.2 ENERGY EFFICIENCY IN A D2D NETWORK

Aiming at improving the energy efficiency, and at the same time providing higher spectral efficiency in the network, the direct communication between devices is seen as a possible candidate for machine-type communications (MTC) scenarios within 5G communication networks (DOPPLER et al., 2009). Such D2D deployment may be able to alleviate the network traffic at the BSs, while requiring less transmit power to communicate in a dense scenario, where links between neighbor devices are shorter (DOPPLER et al., 2009).

In particular, (Lien et al., 2016) show us insights of a D2D network communication based on 3GPP release 12 standard. Thus, the standard proposal is public safety and not a commercial or social intent. Anyhow, three scenarios are covered for public safety as in Figure 1: in-coverage scenario where the D2D link is under coverage of a BS; out-of-coverage when the D2D link is out of coverage or all BSs are damaged; and a partial-coverage where the D2D link is partially out of coverage.

Nevertheless, research on D2D communication includes re-using the same spectrum as the conventional cellular network and the unlicensed bands motivated on wider bands and spectrum price. In contrast, in the unlicensed band, there is higher interference, which yields larger energy consumption than in the licensed bands (Lien et

Figure 1 – D2D communication 3GPP release 12 standard is based on proximity service, (1) Black - D2D link in-coverage, (2) Blue link out-of-coverage, (3) Violet - partial-covered.

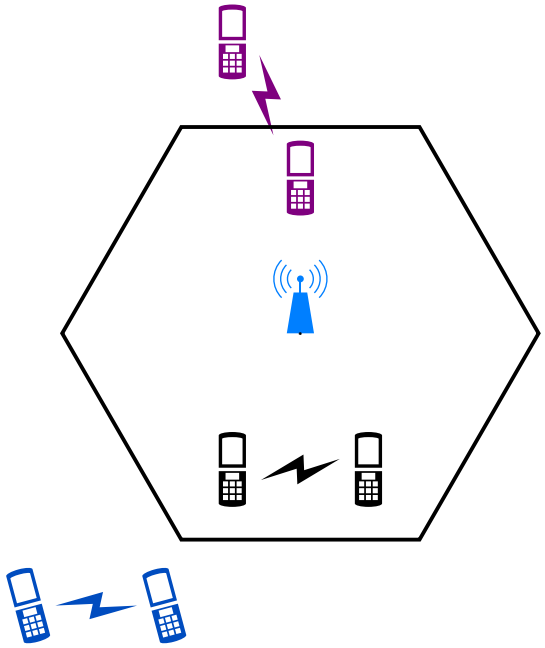

Source: The author

al., 2016).

D2D communication allows two modes of resource allocation, in which either the BS schedules the resource to transmit data and control, or when the D2D user allocates by itself a preconfigured resource to transmit data and control packets (Lien et al., 2016). It is noteworthy that when a D2D link allocates a resource by itself there will be interference according to the number of links nearby. In this sense, with the networks becoming denser, energy efficient solutions for the D2D scenario are important in order to prolong the device's lifetime.

For instance, (PARK; HEATH, 2016) considered a D2D deployment employing MRT techniques, considering multiple antennas at the transmitter and single-antenna receivers. However, the higher rates are followed by an increased energy consumption due to the multiple RF chains used for data transmission. Consequently, approaches based on AS have gained considerably attention from the energy efficiency point of view, once selecting one out of many antennas may yield the same diversity gains of MIMO, but with much lower energy consumption at the RF circuit level (MEHTA et al., 2012). Nevertheless, a performance penalty in terms of higher outage probability comes at the cost of such lower energy consumption (BRANTE et al., 2013). As the D2D communication needs full spectrum for high data rates we analyze the performance under

the interference of multiple nodes, where other concurrent transmitters are distributed following a homogeneous Poisson point process (PPP), which allows us to study an average behavior over an specified area. Then, in order to provide a suitable PCM for the D2D setup we combine (CUI et al., 2005) and (ROSAS et al., 2016), targeting MIMO sensor networks.

In chapter 3 we analyze the energy efficiency of a D2D communication network, employing AS and MRT in a network modeled following PPP (LEE et al., 2016; PARK; HEATH, 2016), which are the two schemes that present the most interesting trade-offs in this particular scenario.

Our main contribution is to show that the MRT technique outperforms the AS in terms of spectral efficiency. On the other hand, AS has increased performance in terms of energy efficiency for short distances, which is typical for D2D deployments, even when MRT employs a theoretically infinite number of feedback bits.

Contribution associated with this chapter can be found in (Krauss et al., 2019).

1.3 GOALS

1.3.1 General Goal

The general goal of this work is to maximize the energy efficiency in modern communication scenarios, consisting of SBSs and D2D devices, combining AS techniques and realistic PCM for each network.

1.3.2 Specific Goals

- In a scenario consisting of SBSs, we aim at modeling the downlink area energy efficiency by resorting to a PCM that includes the RF chains power consumption, SBS specific components and the backhaul power consumption;
- To compare the performance of AS, MRT and SM techniques in terms of energy consumption and area energy efficiency;
- To identify the effect of different PCMs as a function of the area energy efficiency versus area throughput;
- In a D2D network, we aim at employing MIMO techniques in a network setup

modeled by a homogeneous PPP, in order to take the concurrent transmission of other D2D pairs into account;

- To compare the performance in terms of energy efficiency with respect to the main link distance, the number of bits of feedback, the SNR employed and the number of transmit antennas;

2 ENERGY EFFICIENCY OF MULTIPLE ANTENNA CELLULAR NETWORKS IN BASE STATIONS

Some recent studies analyze the energy efficiency of a few MIMO schemes. For instance, in the context of large-scale communications systems, the work in (LI et al., 2014) assessed the energy efficiency performance of AS when two different cases are considered: i.) when the circuit power consumption is comparable to or even dominates the transmit power; and ii.) when the circuit power can be ignored due to relatively much higher transmit power. Then, their analysis shows an optimal number of antennas to maximize the energy efficiency in the first case, whereas in the second case, the energy efficiency is maximized when all the available antennas are used. Furthermore, (HEI et al., 2018) investigates the trade-off between energy efficiency and spectral efficiency in large-scale MIMO systems. As their results show, in order to find Pareto optimal solutions, both energy efficiency and spectral efficiency can be maximized with proper transmit power allocation and optimization on the number of employed antennas.

Moreover, a cross layer approach to the energy efficiency has been carried out in (OKUMU; DLODLO, 2017), which takes physical and link layers into account. Then, by comparing SM and AS, the authors provide algorithms to optimize the number of active antennas and the transmit power in this context. In addition, (WANG; VANDENDORPE, 2017) studies the mathematical property of the energy efficiency as a function of the number of antennas. The authors prove that the monotonicity of the energy efficiency function is guaranteed if the system signal-to-noise ratio (SNR) is greater than a given threshold. Then, a low complexity algorithm to select the optimal number of antennas is proposed.

Common to the above is that the analyses in (JIANG; CIMINI, 2012; LI et al., 2014; HEI et al., 2018; OKUMU; DLODLO, 2017; WANG; VANDENDORPE, 2017) are only performed from a point-to-point communication perspective, which may considerably change in a dense network scenario. Then, the authors in (HERNANDEZ-AQUINO et al., 2015) consider the downlink of a cellular network, where the locations of the BSs are modeled by a PPP. The energy efficiency of the system is obtained for different antenna configurations under various MIMO schemes. Then, expressions for the coverage, throughput, and power consumption are used to formulate the resource allocation problem for each diversity scheme, with the aim of maximizing the network-wide energy efficiency, while satisfying a minimum QoS constraint.

In addition, when analyzing energy efficiency, it was shown that considering a

realistic PCM is important and could lead to contrasting results if the model is not adequately selected (AUER et al., 2011b; RAYEL et al., 2014; HELIOT et al., 2012; RICHTER et al., 2010). A realistic PCM should not only take the transmit power into account, but also several other components that consume power in a BS, such as the AC-DC main power unit, cooling and DC-DC power supplies, as well as the RF power amplifier chain for communications. Additionally, in (TOMBAZ et al., 2014, 2011) it was shown that the power consumed by the backhaul – *i.e.*, the power consumed by the aggregation switches, which is a function of the network traffic – should not be neglected in a complete network energy efficiency evaluation as it may actually be the bottleneck in terms of energy consumption.

For instance, in order to extend coverage in indoor environments or to increase the AEE, a higher number of BSs could be deployed, leading to a denser network. Nevertheless, severe inter-cell interference may arise due to that, and this problem could be addressed with a interference control techniques as the inter-cell interference coordination (ICIC), which was introduced in 3GPP LTE standard release 8 (BOUJELBEN et al., 2014), to allocate different frequency resources to the UEs at the cell edge. Since then, the following LTE releases have improved the interference control techniques, with an *enhanced* ICIC scheme being introduced by releases 9 and 10 (BOUJELBEN et al., 2014), allocating different subframes between macro and small cells, while release 11 has introduced a coordinated multi-point transmit and reception (CoMP) approach (NAGATA et al., 2013), with dynamic coordination for transmission and reception of signals at multiple cells. With CoMP, one or more BSs can serve one UE in order to mitigate interference and to achieve higher throughputs.

However, the use of CoMP relies on a interference control scheme and so they can be used to further instrument interference cancellation schemes. Yet, interference control in addition of an interference cancellation scheme may also be inaccurate for total interference cancellation, because they count on some accuracy level in terms of CSI. With high CSI accuracy, the scheduling among users and BSs can be optimally designed (SUN et al., 2015), achieving high diversity gains. Nevertheless, acquiring accurate CSI in a dense scenario is challenging, so that many sub-optimal quantization approaches are commonly employed (LOVE et al., 2008; KOUNTOURIS; ANDREWS, 2012). As a consequence, since the transmit precoding has the function of suppressing the interference, imperfections in channel estimation may lead to different levels of interference cancellation (SUN et al., 2015). In addition, depending on the size of the cluster controlled by the CoMP technique, some residual inter-cell interference may still persist even with

perfect CSI (SUN et al., 2015). In any case, CSI must be constantly shared between UEs and BSs in order to make scheduling possible, which due to imperfections in channel estimation and the number of served UEs may lead to different levels of interference cancellation.

In this chapter, we analyze the energy efficiency of SM, MRT and AS in the downlink of a cellular network consisting of SBSs, constrained to a minimum received power for the users at the cell edge. Typically, SBSs employ a maximum transmit power of 38 dBm, which is less than the power that can be used by a macro BS, as depicted by (AUER et al., 2011a). In this scenario, the UE is subjected to interference from other neighbor SBSs. We assume that interference may not be fully canceled due to, *e.g.*, the interference mitigation technique or imperfect CSI estimation, so that we consider a fraction of residual interference denoted by κ, which may also reduce the energy and spectral efficiency in dense deployments (FAHAD et al., 2013). Moreover, we employ a realistic PCM that combines (RAYEL et al., 2014) and (TOMBAZ et al., 2011), *i.e.*, it scales with the number of active antennas at the SBS for the different MIMO techniques (RAYEL et al., 2014), at the same time, it includes the backhaul power consumption (TOMBAZ et al., 2011). Due to the consideration in our analysis that the interference may not be fully canceled, and due to the employment of a realistic PCM, we observe different trade-offs in terms of AEE between the MIMO techniques when compared to the results presented in (AUER et al., 2011b; HELIOT et al., 2012; RICHTER et al., 2010). We analyze several scenarios including variations on the demanded capacity, number of antennas, interference level and area to be covered. We show that the AEE can be maximized by a proper selection of the system deployment parameters.

The contributions of this chapter can be summarized as follows:

- We observe different trade-offs in terms of AEE between the MIMO techniques than those found in (AUER et al., 2011b; HELIOT et al., 2012; RICHTER et al., 2010). For instance, AS stands out with the largest AEE when the demand for system capacity is low and the inter-cell interference is not fully canceled, while SM becomes more energy efficient when the capacity demand is larger or when there is full interference cancellation;
- We also show that the energy efficiency results can be significantly different depending on the employed PCM, *e.g.*, if the backhaul or the fraction that scales with the number of antennas are considered or not, it could lead to an unrealistic performance prediction;

- We observe that, as the number of antennas increases, AS becomes the most energy efficient scheme, as its AEE only increases with the number of antennas, whilst SM and MRT have an optimal performance when a 4×4 scheme is considered. Moreover, by fixing the number of BSs and varying the area to be covered, we show that AS is the most energy efficient scheme for a low interference level.

- We emphasize that when AS is the most energy efficient scheme, it always needs more SBSs to achieve the same area throughput as SM, since its multiplexing gain is smaller. Thus, the trade-off between the capital expenditure (CAPEX) for network deployment and the energy savings need to be taken into account by the stakeholders;

- Finally, the performance in terms of AEE is shown to be strongly dependent on κ, so that conclusions in terms of which MIMO scheme achieves the largest AEE may change with the performance of the interference mitigation technique in use.

2.1 SYSTEM MODEL

Let us consider a cellular network composed by hexagonal cells of radius R, covering an area of A km^2, as illustrated in Figure 2. Then, the number of required SBSs can be written as

$$N_{\mathrm{BS}} = \frac{2A}{3\sqrt{3}R^2}. \tag{1}$$

In the downlink direction, the signal transmitted by the SBS and received by the UE is given by (GOLDSMITH, 2005)

$$\mathbf{y} = \sqrt{\frac{P_{\mathrm{L}}\, P_{\mathrm{tx}}}{\widehat{m}_{\mathrm{t}}}}\, \mathbf{H}\, \mathbf{x} + \mathbf{w}, \tag{2}$$

where P_{tx} is the transmit power of the SBS, $\mathbf{H} \in \mathbb{C}^{m_{\mathrm{r}} \times \widehat{m}_{\mathrm{t}}}$ is the channel matrix composed by the fading coefficients $h_{i,j}$, where m_{t} is the number of transmit antennas, $\widehat{m}_{\mathrm{t}}$ is the number of *active* transmit antennas, m_{r} is the number of receiving antennas, $\mathbf{x} \in \mathbb{C}^{\widehat{m}_{\mathrm{t}} \times 1}$ is the unit energy transmitted symbol vector, $\mathbf{y} \in \mathbb{C}^{m_{\mathrm{r}} \times 1}$ is the received symbol vector and $\mathbf{w} \in \mathbb{C}^{m_{\mathrm{r}} \times 1}$ is the zero-mean additive white Gaussian noise with variance $N_0/2$ per dimension, where N_0 is the thermal noise power spectral density per Hertz. Also, without loss of generality, we consider $m_{\mathrm{t}} = m_{\mathrm{r}}$ throughout this chapter, which we denote by

Figure 2 – System model of a cellular network composed by N_{BS} hexagonal cells of radius R, covering an area A.

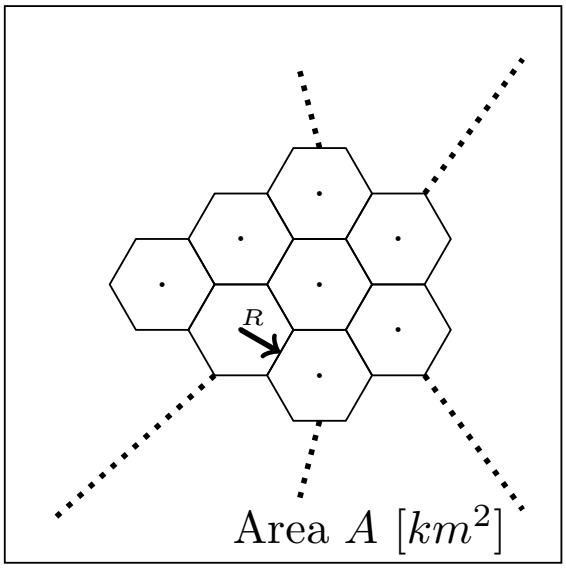

Source: The author

number of antennas.[1] [2]

Moreover, the path-loss is (GOLDSMITH, 2005)

$$P_{\mathrm{L}} = \frac{G\lambda^2}{L(4\pi)^2 d^{\alpha}}, \tag{3}$$

where α is the path loss exponent in a urban microcells environment, d is the transmission distance, G is the antenna gain, L is the link margin and λ is the wavelength.

Then, the average SNR at the receiver is

$$\overline{\gamma} = \frac{P_{\mathrm{L}} P_{\mathrm{tx}}}{N_0 W}, \tag{4}$$

where $W$is the channel bandwidth.

Moreover, we also consider that the communication links are subjected to interference, which may not be fully canceled depending on the employed interference mitigation scheme, so that in our model we include a factor denoted by $\kappa \in [0,1]$ that multiplies the maximum interference power P_{I}. Where P_{I} is the interference power from neighboring cells. In this scenario all neighboring BSs are assumed to have the same transmit power, without frequency reuse, in order to perform a worst case analysis.

[1] Notice that $\widehat{m}_{\mathrm{t}} \leq m_{\mathrm{t}}$, while the active antennas are selected according to the employed MIMO transmission scheme.

[2] In addition, throughout this chapter we assume that the UE have m_{r} antennas that will always remain active.

Therefore, each user considered at the cell edge will suffer interference from other BSs. Thus, the signal-to-interference power ratio (SIR) in the case of hexagonal cells becomes (GOLDSMITH, 2005)

$$\zeta = \frac{P_{\mathrm{L}} P_{\mathrm{tx}}}{\kappa P_{\mathrm{I}}}, \tag{5}$$

in which $\kappa = 0$ yields $\zeta \to \infty$, *i.e.*, full interference cancellation, while $\kappa = 1$ considers the worst-case scenario with no interference cancellation at all.

The average SINR for the UE at the cell edge for the sch scheme is

$$\epsilon_{\mathrm{sch}} = \frac{P_{\mathrm{L}} P_{\mathrm{tx}}}{N_0 W + \kappa P_{\mathrm{I}}} = \frac{\overline{\gamma}}{1 + \overline{\gamma}\, \zeta^{-1}}. \tag{6}$$

where $\mathrm{sch} \in \{\mathrm{MRT}, \mathrm{AS}, \mathrm{SM}\}$.

2.1.1 Network Total Power

To compute the network total power consumption, P_{net}, we employ a PCM combining (RAYEL et al., 2014) and (TOMBAZ et al., 2011), which also takes into account the number of active antennas at the SBS. Thus,

$$P_{\mathrm{net}} = N_{\mathrm{BS}} \left[\widehat{m}_{\mathrm{t}} (\psi P_{\mathrm{tx}} + P_1) + P_2 \right] + P_{\mathrm{bh}}, \tag{7}$$

where ψ is a constant that encompasses the effects of the power amplifier drain efficiency, cooling, power supply and battery backup losses, P_1 represents the part of the circuitry power consumption that grows linearly with $\widehat{m}_{\mathrm{t}}$, while P_2 is the power consumption that does not depend on $\widehat{m}_{\mathrm{t}}$ (RAYEL et al., 2014; AUER et al., 2011b). Moreover, P_{bh} is the power consumption of the backhaul[3].

Furthermore, as depicted in Figure 3, the power consumed by the backhaul takes into account the power consumed by the downlink interfaces (P_{dl}), dedicated to each BS, the uplink interfaces (P_{ul}), dedicated to each access switch, and the power consumed by the access switch (P_{s}), being written as (TOMBAZ et al., 2011)

$$P_{\mathrm{bh}} = \left\lceil \frac{N_{\mathrm{BS}}}{\max_{\mathrm{dl}}} \right\rceil P_{\mathrm{s}} + N_{\mathrm{BS}} P_{\mathrm{dl}} + N_{\mathrm{ul}} P_{\mathrm{ul}}, \tag{8}$$

where $\lceil . \rceil$ is the ceil operation, $\max_{\mathrm{dl}}$ is the maximum number of downlink interfaces available in an aggregation switch and $N_{\mathrm{ul}} = \left\lceil \frac{Ag_{\mathrm{tot}}}{U_{\max}} \right\rceil$ is the number of uplink interfaces (number of ports used by the switch), where Ag_{tot} is the total traffic aggregated at all

[3]Let us remark that $P_{\mathrm{bh}} = 0$ in (RAYEL et al., 2014), while $P_1 = 0$ in (TOMBAZ et al., 2011).

Figure 3 – Backhauling Layout. The Radio Remote Units (RRUs) are connect via wireless channel to the Baseband Units (BBUs). Then, the optical backhaul consists of 1 Gbps SFPs (Small Form-Factor Pluggable) connected to the access switch, by its turn connected through a 10 Gbps interface to the border router.

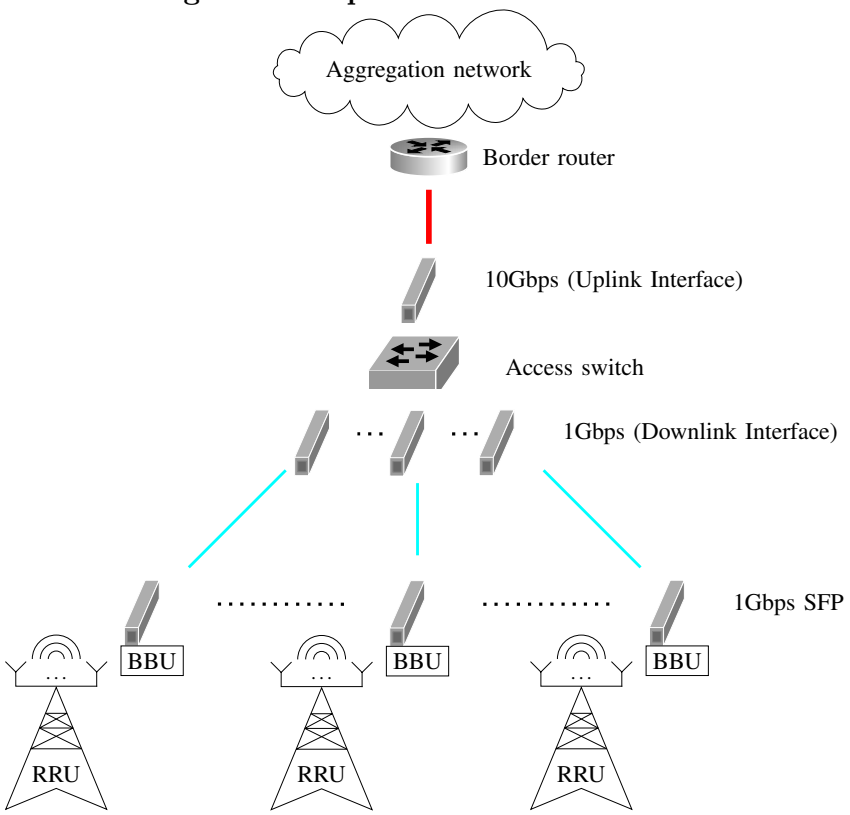

Source: Adapted from (TOMBAZ et al., 2011).

switches (or total traffic generated by all SBS) and $U_{\max}$ is the maximum rate supported by each uplink interface.

In addition, the power consumed by each access switch is (TOMBAZ et al., 2011)

$$P_{\mathrm{s}} = \delta P_{\mathrm{s,max}} + (1-\delta)\frac{Ag_{\mathrm{switch}}}{Ag_{\max}} P_{\mathrm{s,max}}, \tag{9}$$

where $\delta \in [0,1]$ is a weighting parameter, $P_{\mathrm{s,max}}$ is the maximum power consumed by the switch, Ag_{switch} is the traffic traversing the switch, and $Ag_{\max}$ is the maximum traffic supported by the switch. It is worth noting that the term $Ag_{\mathrm{switch}}/Ag_{\max}$ in (9) expresses the percentage of traffic transversing the switch, which is related to the number of ports that are occupied.

2.1.2 Area Energy Efficiency

In order to compare networks with different cell sizes, we define the area power consumption in W/km^2 as (TOMBAZ et al., 2014)

$$\Omega = \frac{P_{\text{net}}}{A}, \tag{10}$$

while we also assume that the cells may have different area throughput targets, which can be written as (TOMBAZ et al., 2011)

$$\tau_{\text{sch}} = \frac{C_{\text{net}}^{(\text{sch})}}{A}, \tag{11}$$

where $C_{\text{net}}^{(\text{sch})}$ is the total network capacity for the sch scheme, which is different depending on the employed MIMO scheme, as will be detailed in Section 2.2. Finally, to reflect the ratio between the overall network capacity and the energy consumption, we adopt an AEE metric for sch, in bits/J/km^2, given by (SHAHAB; ZAINUN, 2015)

$$\eta_{\text{sch}} = \frac{\tau_{\text{sch}}}{P_{\text{net}}}. \tag{12}$$

2.2 MIMO TRANSMISSION SCHEMES

In this section, we define the SNR and the network capacity for three MIMO schemes, namely spatial multiplexing, maximal ratio transmission and transmit antenna selection. Moreover, let us remark that we restrict our investigation to techniques that are available in current deployments, especially for SBSs, and we leave other approaches such as Massive MIMO (BJORNSON et al., 2015) for future investigations.

2.2.1 Spatial Multiplexing (SM)

In order to exploit the multiplexing gains provided by multiple antennas, SM transmits $m = \min\{m_{\text{t}}, m_{\text{r}}\}$ independent and separate encoded data streams, one by each transmit antenna[4]. Then, the average SNR per receive antenna $\overline{\gamma}_{\text{sch}}$ is (RAYEL et al., 2014)

$$\overline{\gamma}_{\text{SM}} = \frac{\overline{\gamma}}{m}, \tag{13}$$

[4]In the SM and MRT schemes we consider that all transmit antennas are active ($\widehat{m}_{\text{t}} = m_{\text{t}}$).

while the capacity of the SM scheme is (RAYEL et al., 2014; KHAN et al., 2016)

$$C_{\text{net}}^{(\text{SM})} = N_{\text{BS}}\, W\, \log_2\left[\det\left(\mathbf{I}_m + \frac{\overline{\gamma}_{\text{SM}}\, \boldsymbol{\Xi}}{1+\overline{\gamma}_{\text{SM}}\, \zeta^{-1}\, \boldsymbol{\Xi}}\right)\right], \tag{14}$$

where $\mathbf{I}_m$ is an $m \times m$ identity matrix and $\boldsymbol{\Xi} \in \mathbb{C}^{m\times m}$ corresponds to a random matrix given by

$$\boldsymbol{\Xi} = \begin{cases} \mathbf{H}\mathbf{H}^{\dagger} & m_{\text{t}} \geq m_{\text{r}} \\ \mathbf{H}^{\dagger}\mathbf{H} & m_{\text{t}} < m_{\text{r}} \end{cases}, \tag{15}$$

with $\mathbf{H}^{\dagger}$ being the conjugate transpose of $\mathbf{H}$.

2.2.2 Maximal Ratio Transmission (MRT)

Differently from SM, MRT exploits channel knowledge at the transmitter and at the receiver in order to mitigate the effects of fading (MCKAY et al., 2006). Thus, the same symbol is transmitted over all m_{t} antennas, so that the instantaneous SNR γ_{sch} at the receiver is

$$\gamma_{\text{MRT}} = \overline{\gamma}\, \lambda_{\max}, \tag{16}$$

where $\lambda_{\max}$ is the maximum eigenvalue of $\boldsymbol{\Xi}$ in (15).

Then, the capacity for the MRT technique is given by (MCKAY et al., 2006; RAYEL et al., 2014)

$$C_{\text{net}}^{(\text{MRT})} = N_{\text{BS}}\, W\, \log_2\left(1 + \frac{\gamma_{\text{MRT}}}{1+\zeta^{-1}\, \gamma_{\text{MRT}}}\right). \tag{17}$$

2.2.3 Antenna Selection (AS)

When AS is employed, we assume that only $\widehat{m}_{\text{t}} = 1$ antenna is selected from the set of m_{t} transmit antennas, which saves power since only one RF chain remains active. Here we assume maximum ratio combining (MRC) at the receiver side, so that the instantaneous SNR is (GOLDSMITH, 2005)

$$\gamma_{\text{AS}} = \overline{\gamma} \max_i \sum_{j=1}^{m_{\text{r}}} |h_{i,j}|^2, \tag{18}$$

where the maximum over i represents that only the best antenna of the transmitter is chosen, while the sum comes from the MRC at the receiver.

Thus, the capacity of AS yields

$$C_{\text{net}}^{(\text{AS})} = N_{\text{BS}}\, W\, \log_2\left(1+\frac{\gamma_{\text{AS}}}{1+\zeta^{-1}\,\gamma_{\text{AS}}}\right). \tag{19}$$

2.3 NUMERICAL RESULTS AND DISCUSSION

In this section, a few numerical results are presented. The simulation parameters are shown in Table 1, according to (TOMBAZ et al., 2014), with the constants regarding SBS power consumption based on (RAYEL et al., 2014; HELIOT et al., 2012) and with the power consumption parameters associated with the backhaul following (TOMBAZ et al., 2011).

Table 1 – System Parameters for Small Base Station Network.

Parameter	Description	Value
A	Coverage area	40 km^2
G	Antenna gain	10 dBi
L	Link margin	10 dB
α	Path-loss exponent	3.5
$P_{\min}$	Minimum power requirement at cell edge	-100 dBm
f	Carrier frequency	2.5 GHz
W	Bandwidth	5 MHz
N_0	Noise psd/Hz	-174 dBm/Hz
$P_{\max}$	Maximum power constraint at cell edge	6.31 W
ψ	Constant for power consumption	3.14
P_1	Power consumption dependent of $\widehat{m}_{\text{t}}$	35 W
P_2	Power consumption not dependent of $\widehat{m}_{\text{t}}$	34 W
$U_{\max}$	Maximum rate at each uplink interface	10 Gbps
δ	Weighting parameter	0.9
$\max_{\text{dl}}$	Maximum number of downlink interfaces	24
$Ag_{\max}$	Maximum traffic per switch	24 Gbps
$P_{\text{s,max}}$	Maximum power consumed by the switch	300 W
P_{ul}	Power consumed by uplink interfaces	2 W
P_{dl}	Power consumed by downlink interfaces	1 W

Source: According to (TOMBAZ et al., 2014; RAYEL et al., 2014; HELIOT et al., 2012; TOMBAZ et al., 2011)

2.3.1 Area Power Consumption

Let us first analyze the area power consumption (Ω) as a function of the area throughput (τ_{sch}). For each scenario, there is a minimum N_{BS} required to cover the area

Figure 4 – Area power consumption (Ω) as a function of the area throughput (τ_{sch}), varying N_{BS}, with $m_{\text{t}} = m_{\text{r}} = 2$.

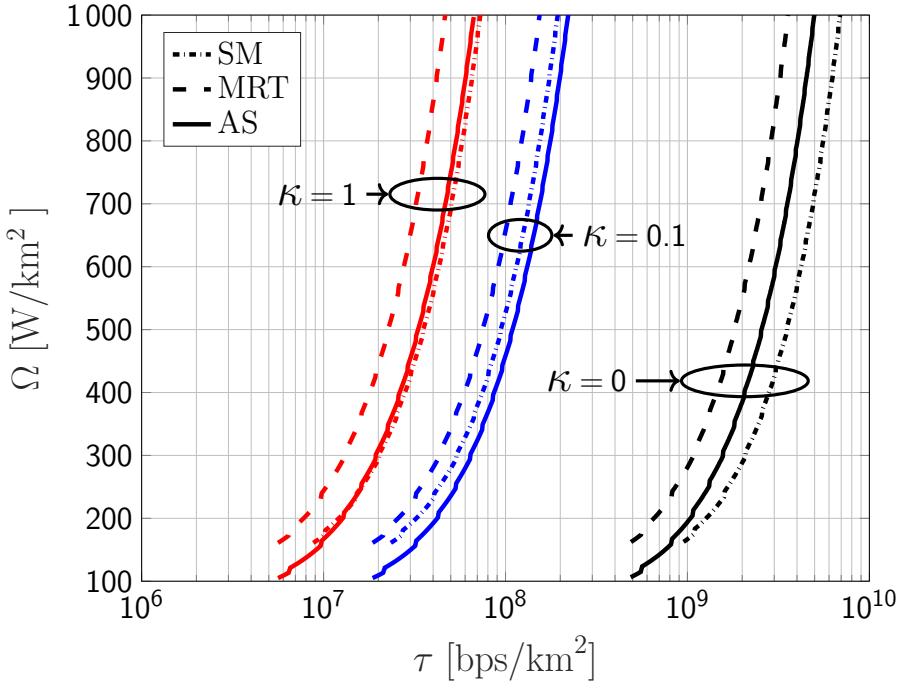

Source: The author

Figure 5 – Number of SBSs (N_{BS}) as a function of the area throughput (τ), with $m_{\text{t}} = m_{\text{r}} = 2$ and $\kappa = 0$.

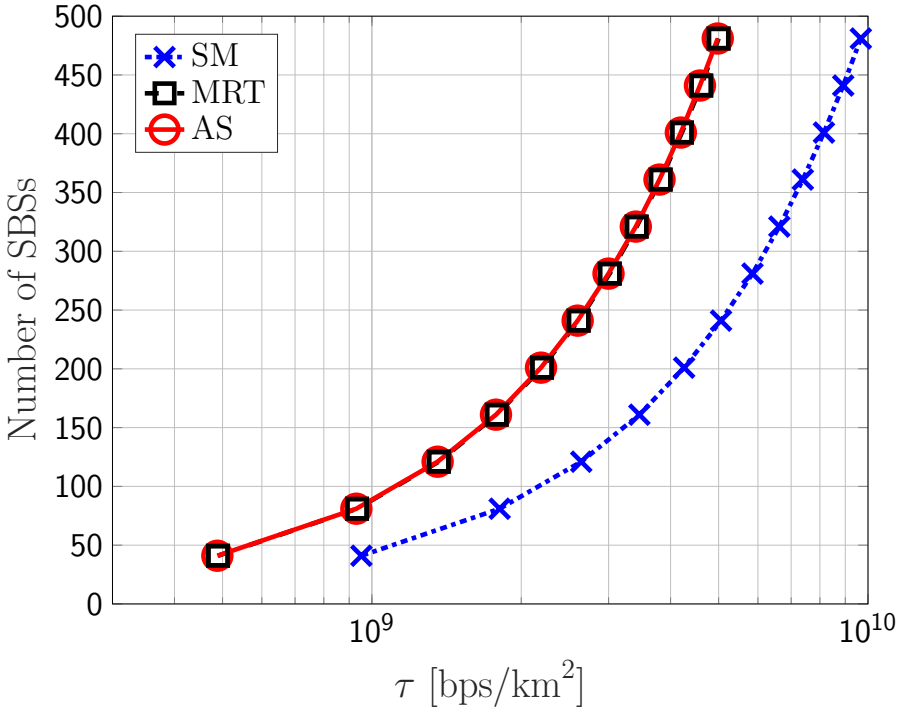

Source: The author

A, which is obtained respecting the maximum transmit power $P_{\max}$ for each SBS, while guaranteeing a minimum received power $P_{\min}$ for the UEs at the cell edge. Moreover, we also consider that a maximum of $N_{\mathrm{BS,max}} = 500$ can be deployed, which is the result of applying the parameters from Table 1 into (1). In addition, notice that all Figures of this chapter start with a minimum number of N_{BS} due to $P_{\min}$ constraint from Table 1.

Figure 4 plots Ω as a function of τ_{sch} in the case that only SBSs are employed. From the figure, we can notice that AS minimizes the area power consumption when $\kappa > 0$. Only when there is no interference at the cell edge ($\kappa = 0$), SM performs better than AS due to the multiplexing gains that provide the required system capacity. However, when κ increases, the higher SNR provided by SM affects both the numerator and denominator of the SINR in (14), so that the smaller number of active RF chains yields the lowest area power consumption for the AS scheme.

The analysis of Figure 4 is complemented by Figure 5, showing the number of employed SBSs (N_{BS}) as a function of τ_{sch}. As we can see, MRT and AS employ the same N_{BS}, which corroborates with the results in (RAYEL et al., 2014) showing that the capacity of the MRT scheme is only slightly larger than that of AS. Then, the higher area power consumption of MRT with respect to AS in Figure 4 comes mainly due to the increased power consumption of the antenna RF chains. By its turn, N_{BS} is considerably decreased for the SM scheme due to the multiplexing gains, especially at high τ_{sch}.

Moreover, an interesting behavior caused by the backhaul power consumption is displayed in Figure 6. According to (9), when a new switch must be turned on to support the traffic demand through the backhaul, 90% of $P_{\mathrm{s,max}}$ is consumed (due to the term δ in Table 1), which is higher than the power consumption of the network (P_{net}) in the case of SBS. Thus, the curves exhibit a slight saw shape, indicating when a new switch starts.

2.3.2 Area Energy Efficiency

In this subsection, we analyze the AEE (η) as a function of τ_{sch}, with $m_{\mathrm{t}} = m_{\mathrm{r}} = 2$. First, in Figure 6, η is evaluated in a scenario where the interference is considered to be fully canceled ($\kappa = 0$). As we can observe, AS performs better than MRT, while SM has the best performance in this particular scenario. In addition, "$\leftarrow \bullet$" indicates the N_{BS} employed by SM, "$\leftarrow \times$" the N_{BS} employed by AS and "$\leftarrow$ o" the N_{BS} employed by MRT.

Next, Figure 7 presents the same analysis as in Figure 6, but considering that $\kappa = 0.1$ (interference is not fully canceled) and $\kappa = 1$ (no interference cancellation at all).

Figure 6 – Area energy efficiency (η) as a function of the area throughput (τ) for SBSs with $m_{\mathrm{t}} = m_{\mathrm{r}} = 2$ and $\kappa = 0$. The arrow "$\leftarrow \bullet$" indicates the N_{BS} employed by SM, "$\leftarrow \times$" the N_{BS} employed by AS and "$\leftarrow$ o" the N_{BS} employed by MRT.

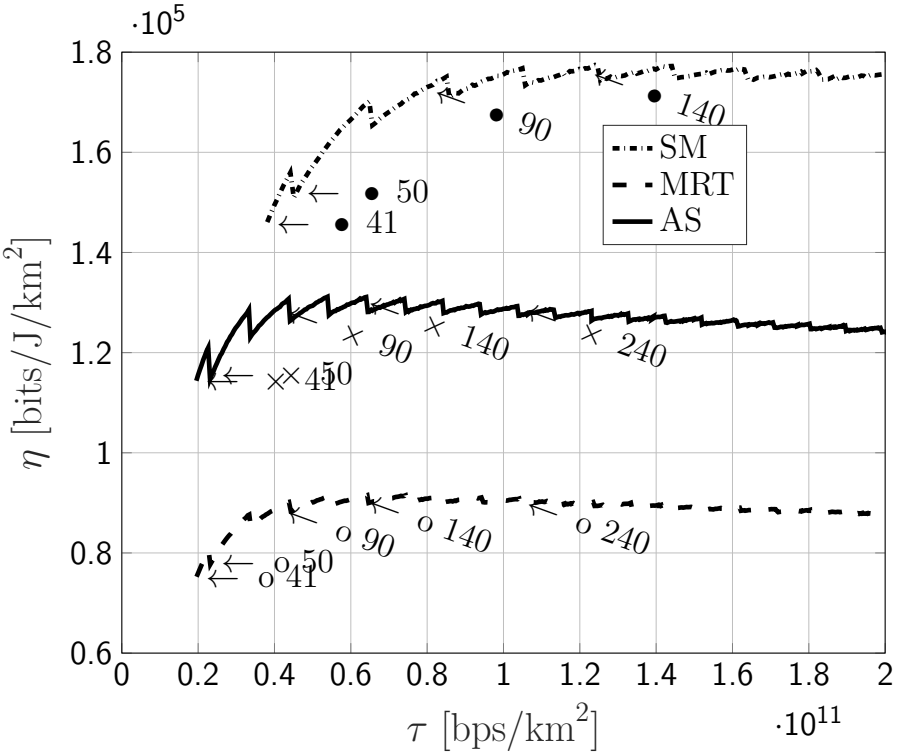

Source: The author

As we can observe, this analysis corroborates with the results of Figure 4, so that AS achieves the best performance when $\kappa = 0.1$. In this case, it is interesting to notice that when a fixed N_{BS} is chosen for $\kappa = 0.1$, AS is more energy efficient than SM and MRT, but SM yields a higher area throughput. Furthermore, the same intersection between AS and SM is observed when $\kappa = 1$, so that AS has higher η when $\tau < 526$ Mbps/km^2, while SM performs better when τ_{sch} increases. Finally, it is also worth noting from Figures 6 and 7 that even when AS is more energy efficient than SM, it requires a higher number of deployed SBSs.

2.3.3 Different Power Consumption Models

The effect of different PCMs is illustrated in Figure 8, where we only compare the AEE of SM and AS for the sake of a better visualization. In the figure, besides the power consumption model depicted by (7), we also consider the models presented by (RAYEL et al., 2014), which does not include the backhaul power consumption (*i.e.*, $P_{\mathrm{bh}} = 0$), and the model in (TOMBAZ et al., 2011), which does not include the fraction of the power

Figure 7 – Area energy efficiency (η) as a function of τ_{sch} for SBSs with $m_{\text{t}} = m_{\text{r}} = 2$ and $\kappa = \{0.1, 1\}$.

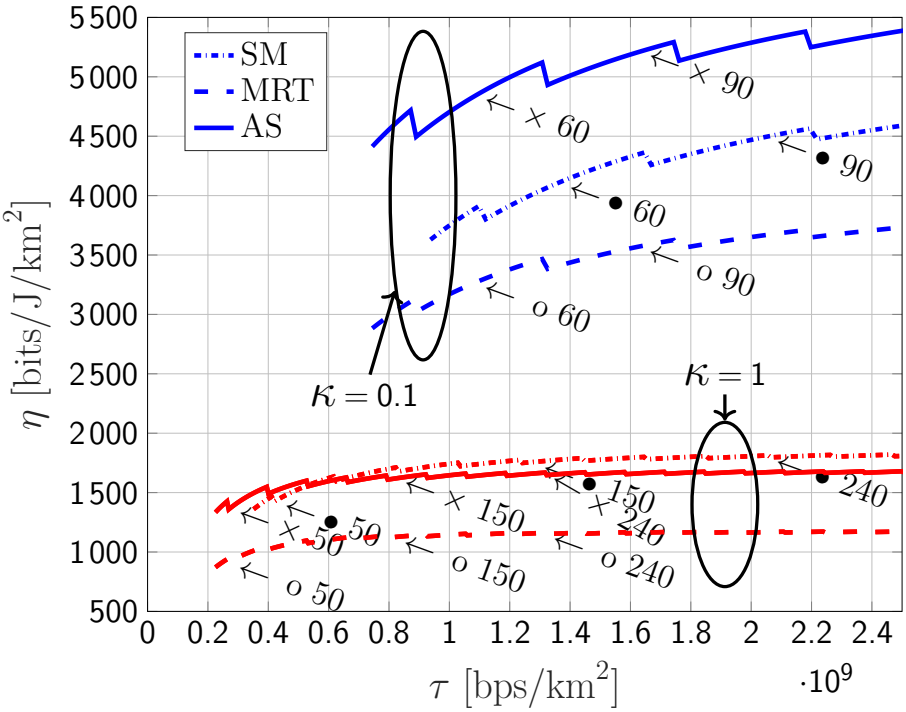

Source: The author

that scales with $\widehat{m}_{\text{t}}$ (*i.e.*, $P_1 = 0$).

As we observe, the intersection between AS and SM changes depending on the considered PCM. For instance, the PCM in (TOMBAZ et al., 2011) yields an optimistic assumption for the energy efficiency, once some fraction of power spent by the SBSs in idle mode is not considered. Moreover, by comparing the PCMs in (7) and that from (RAYEL et al., 2014), we observe that it is crucial to take P_{bh} into account, since it considerably changes the energy efficiency results, which are rather optimistic when $P_{\text{bh}} = 0$.

2.3.4 Fixed Network Capacity and Area Energy Efficiency

Figure 9 evaluates η as a function of the number of antennas ($m_{\text{t}} = m_{\text{r}}$), with $\kappa = 0$ and a target network capacity of $C_{\text{net}} = 10$ Gbits/s. Moreover, the required number of SBSs is calculated for the case when $m_{\text{t}} = m_{\text{r}} = 2$, and it remains fixed while we increase the number of antennas. For instance, $N_{\text{BS}} = 10$ is required by the SM technique when $m_{\text{t}} = m_{\text{r}} = 2$, and $N_{\text{BS}} = 21$ is needed for AS and MRT, which are maintained when we increase $m_{\text{t}} = m_{\text{r}}$ once the goal is to analyze the effect of increasing the number of antennas in an existing network deployment.

Figure 8 – Area energy efficiency (η) as a function of the area throughput (τ) for SBSs with $m_{\mathrm{t}} = m_{\mathrm{r}} = 2$ and $\kappa = 0$.

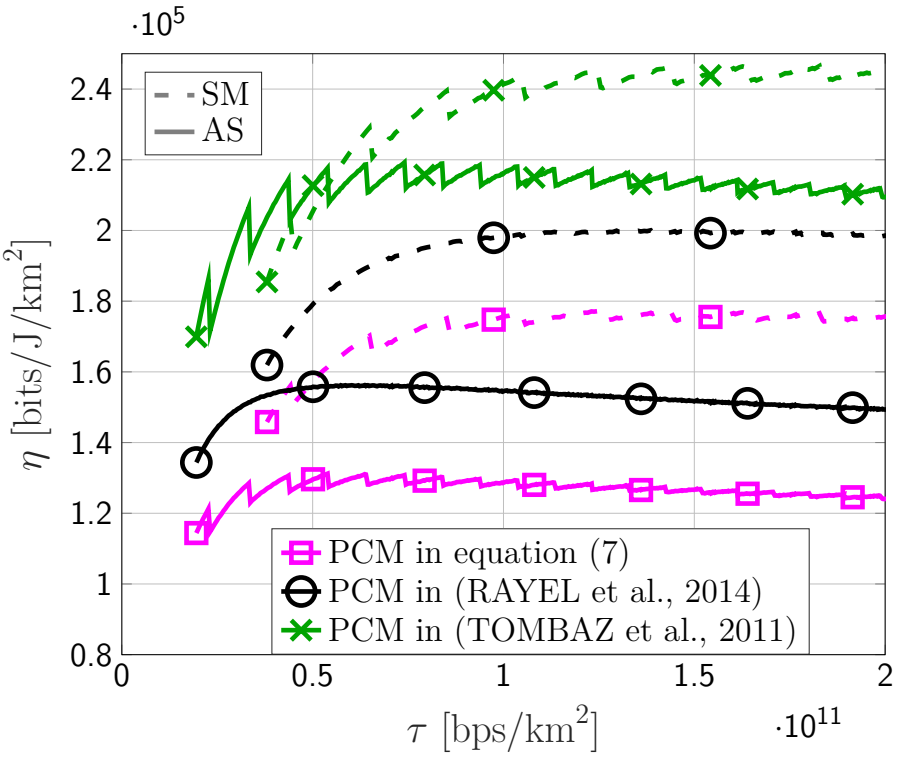

Source: The author

As we observe, SM and MRT exhibit a maximal performance when $m_{\mathrm{t}} = m_{\mathrm{r}} = 4$, which is due to the fact that the energy consumption also scales with the number of antennas, limiting the AEE. On the other hand, the AEE using the AS technique is an increasing function with the number of antennas, although we observe a saturation effect when $m_{\mathrm{t}} = m_{\mathrm{r}} > 10$.

Nevertheless, it is interesting to notice that the performance may change depending on the number of antennas and amount of interference. For instance, Figure 10 plots the AEE as a function of the number of antennas in a scenario without interference cancellation ($\kappa = 1$). As we observe, the performance decreases for SM and MRT when the number of antennas increase, while η is practically constant for the AS scheme. Figure 11 complements the analysis by plotting the area power consumption as a function of the area throughput for $\kappa = 1$ and three different antenna arrangements, with $m_{\mathrm{t}} = m_{\mathrm{r}} = 2$ in Figure 11a, $m_{\mathrm{t}} = m_{\mathrm{r}} = 4$ in Figure 11b, and $m_{\mathrm{t}} = m_{\mathrm{r}} = 8$ in Figure 11c. As the figures show, the performance of AS slightly increases with the number of antennas, while the power consumption for SM and MRT considerably increases. Nevertheless, we also notice that the area throughput achieved by AS with $N_{\mathrm{BS}} = 500$ is still much smaller than that

Figure 9 – Area energy efficiency (η) as a function of the number of antennas ($m_t = m_r$) with $\kappa = 0$, and with a capacity target of 10 Gbits/s and $N_{\mathrm{BS}} = 10$ for SM technique, $N_{\mathrm{BS}} = 21$ for AS and MRT techniques.

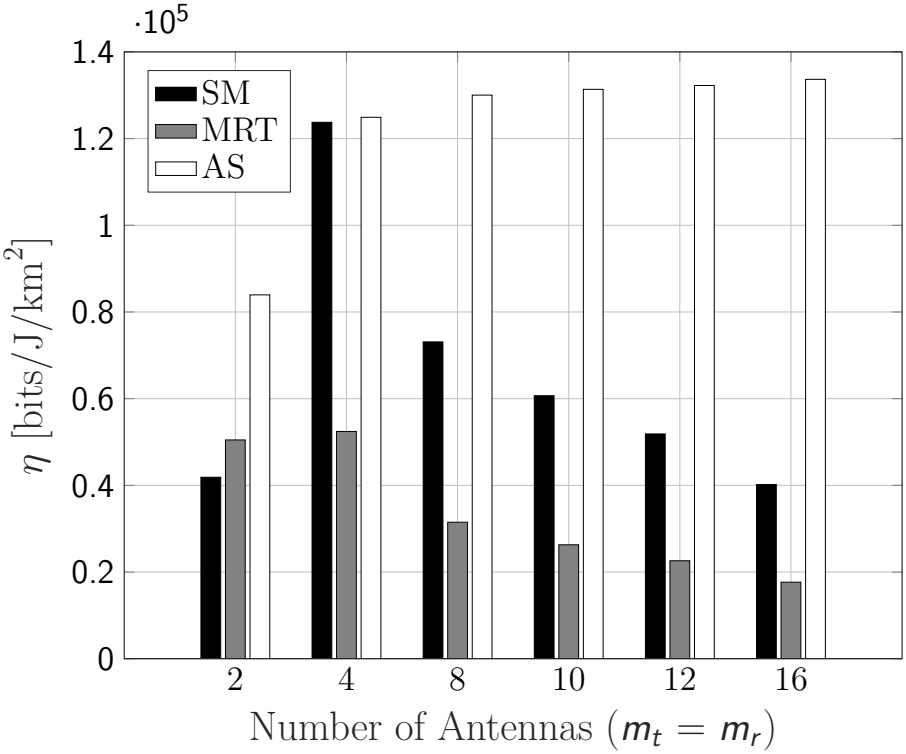

Source: The author

of SM with the same antenna configuration.

Furthermore, Figure 12 evaluates the area power consumption as a function of κ, with $m_{\mathrm{t}} = m_{\mathrm{r}} = 2$ and a target network capacity of $C_{\mathrm{net}} = 7$ Gbits/s. Consistent with Figure 9, AS achieves the highest AEE in this scenario. However, it is interesting to notice that this increased performance comes at the cost of employing more SBSs than SM to supply the same target network capacity.

2.3.5 Area Energy Efficiency for Different Coverage Areas

Finally, we evaluate the AEE for different coverage areas, while maintaining N_{BS} fixed. Then, for different coverage areas, we evaluate the AEE in order to ensure that the users at the cell edge obtain $P_{\mathrm{min}} = -100$ dBm, subjected to the transmit power constraint $P_{\mathrm{tx}} \leq P_{\mathrm{max}}$. In this particular scenario, we consider that $N_{\mathrm{BS}} = 80$ and $m_t = m_r = 2$, with $\kappa = 0.1$ in Figure 13 and $\kappa = 1$ in Figure 14.

As Figure 13 shows, AS outperforms the other schemes in terms of AEE,

Figure 10 – Area energy efficiency (η) as a function of the number of antennas ($m_t = m_r$) with $\kappa = 1$, and with a capacity target of 1 Gbits/s and $N_{\mathrm{BS}} = 117$ for SM technique, $N_{\mathrm{BS}} = 183$ for AS and MRT techniques.

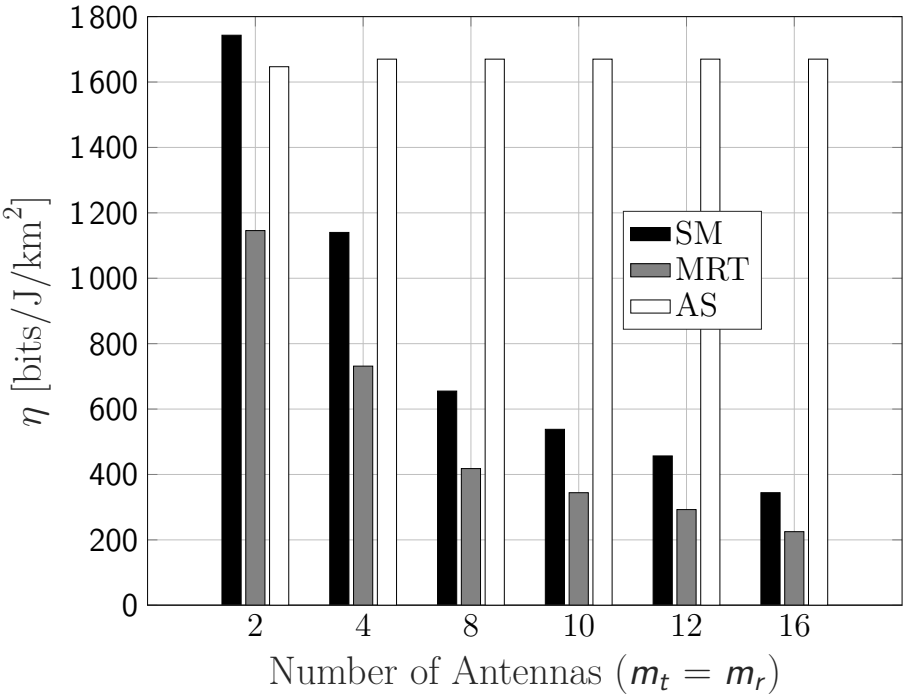

Source: The author

Figure 11 – Area power consumption (Ω) as a function of the area throughput (τ), for different antenna configurations with $\kappa = 1$.

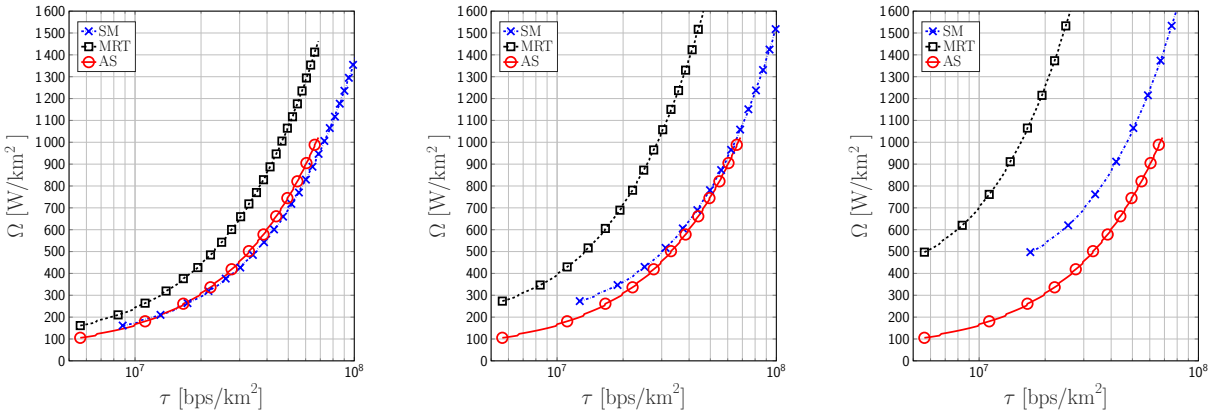

(a) $m_{\mathrm{t}} = m_{\mathrm{r}} = 2$ (b) $m_{\mathrm{t}} = m_{\mathrm{r}} = 4$ (c) $m_{\mathrm{t}} = m_{\mathrm{r}} = 8$

Source: The author

regardless of the coverage area, which corroborates with the results of Figures 4 and 7. Moreover, as the coverage area increases, the coverage radius of each SBS also increases, which demands more transmission power per cell and as a consequence η decreases with A. When $\kappa = 1$, Figure 14 shows a slightly better performance of SM compared to AS

Figure 12 – Area energy efficiency (η) as a function of κ for $m_t = m_r = 2$, and with a capacity target of 7 Gbits/s.

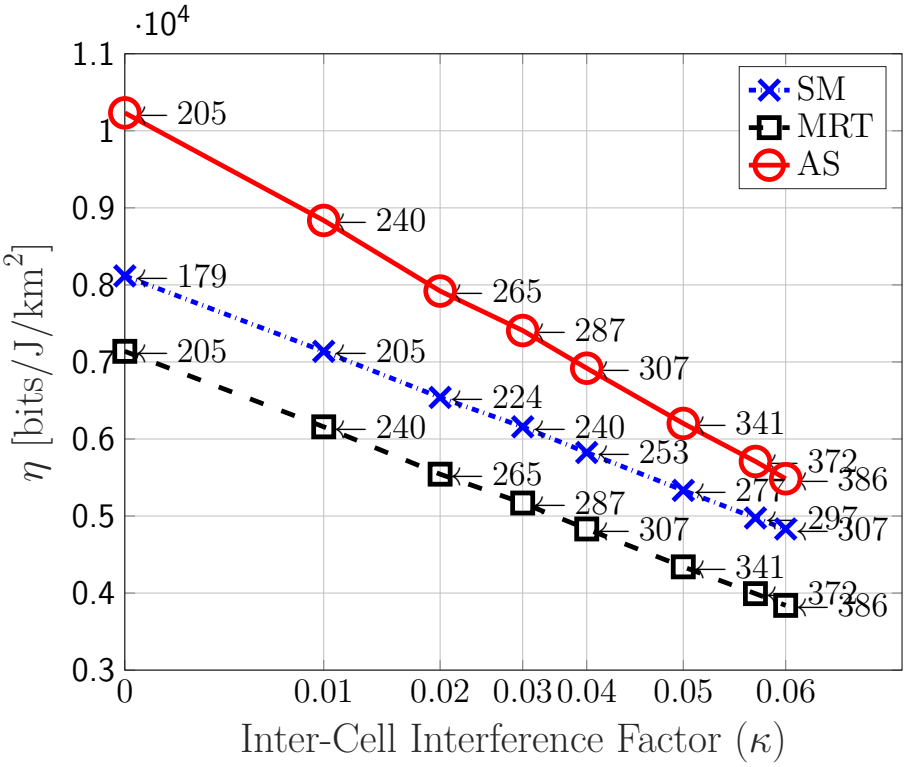

Source: The author

and MRT. Interestingly, the performance of SM and AS in terms of AEE is very similar when $A \geq 40$ km^2, with AS slightly outperforming SM when $A = 70$ km^2.

2.4 CONCLUSIONS

In this chapter, we evaluated a cellular network employing three different multiple antenna techniques: SM, MRT and AS. The goal is to optimize the AEE by calculating the optimal number of SBSs given some requirements, such as demanded network capacity, amount of interference and employed MIMO scheme. Our results show that SM and AS usually achieve the best performance in terms of area power consumption and AEE. For instance, AS performs better when the interference is not fully canceled and for no interference cancellation when the demand for system capacity is lower, while SM becomes more energy efficient when the demanded capacity is higher.

Additionally, when the capacity demand and the area to be covered are fixed, we also show that although achieving the highest AEE, AS also demands more SBSs than SM. Finally, the system performance in terms of AEE is shown to be strongly dependent on the

Figure 13 – Area energy efficiency (η) as a function of the coverage area with $\kappa = 0.1$ and $N_{\mathrm{BS}} = 80$.

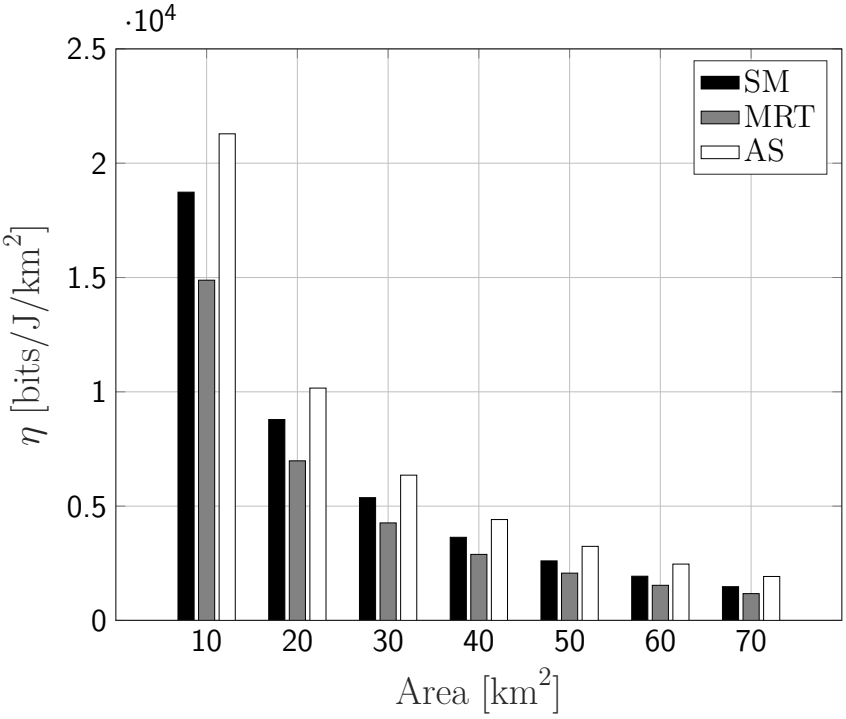

Source: The author

Figure 14 – Area energy efficiency (η) as a function of the coverage area with $\kappa = 1$ and $N_{\mathrm{BS}} = 80$.

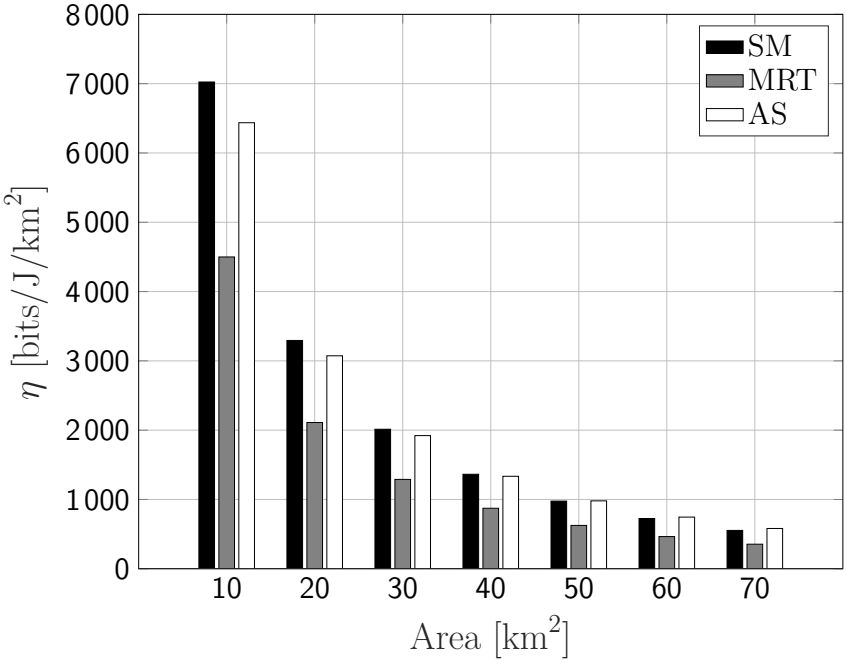

Source: The author

amount of interference, which in turn depends on the employed interference-mitigation scheme, and on the employed PCM, if the backhaul or the fraction that scales with the number of antennas are considered or not.

3 AREA ENERGY EFFICIENCY IN LIMITED FEEDBACK DEVICE-TO-DEVICE NETWORKS

D2D communication is an expected solution to achieve high data rates at local services, possibly alleviating BS data traffic. Therefore, the use of D2D approaches within the 5G context may be able to improve throughput and energy efficiency (SAFDAR et al., 2016). As a consequence,the use of D2D approaches within the 5G context may be able to improve, *e.g.*, in (XU et al., 2016; OSMAN et al., 2017; KAI et al., 2018; HU et al., 2017).

For instance, in (XU et al., 2016) devices are grouped according to a resource allocation policy, based on two constraints: interference and energy efficiency. Then, a distributed iterative algorithm is proposed to maximize the energy efficiency. Moreover, the advantage of a cooperative approach in terms of energy efficiency is investigated by (OSMAN et al., 2017), where three transmission modes are compared: cellular, D2D and cooperative D2D. The results show that either D2D or cooperative D2D modes are advantageous in terms of energy efficiency and data rate, compared to the cellular mode. Yet, a joint optimization of transmit power and subcarrier assignment is proposed in (KAI et al., 2018), whose goal is to minimize the overall energy consumption in a D2D setup. Also, the work in (HU et al., 2017) proposes a resource reuse strategy, aiming at maximizing the energy efficiency of a D2D scenario coexisting with a cellular cell, which outperforms existing schemes for the same scenario.

Hence, in this chapter we focus on the energy efficiency of MIMO techniques for the D2D network scenario. Specifically, we focus on AS and MRT techniques. In addition, we assume that the D2D devices are randomly distributed in space, possibly communicating with their pairs at the same time, which is modeled through a homogeneous PPP (HAENGGI et al., 2009). Afterwards, we derive the ergodic spectral efficiency and area energy efficiency expressions for these schemes, assuming a limited feedback channel consisting of a few bits. Moreover, a realistic PCM representative of sensor networks is employed (CUI et al., 2005) and (ROSAS et al., 2016).

Our results shows that the MRT technique outperforms AS in terms of spectral efficiency, even when admitting same number of feedback bits. On the other hand, AS performs better than MRT in terms of energy efficiency for short distances, even if MRT employs a theoretically infinite number of feedback bits, which is due to the lower energy consumption related to the RF circuitry. Furthermore, we also observe that few antennas are optimal for short distances in both schemes, while the optimal number of antennas

tends to increase with the distance, especially for the MRT scheme. In addition, by optimizing the transmit power we also show that the optimal SNR employed by the AS scheme is always smaller than that of MRT.

3.1 SYSTEM MODEL

Let us assume a D2D communication scenario, illustrated by Figure 15, located in an area A following a homogeneous PPP with density ρ, given in nodes/m^2. In addition, in this chapter we assume that the same number of antennas is deployed at the transmitter and receivers, which we denote by N. This assumption relies on the fact that the same nodes act with both roles in typical D2D scenarios. Moreover, the channel fading is modeled according to a Rayleigh distribution, with the channel matrix composed by independent and identically distributed (i.i.d.) random variables.

Then, we evaluate two different MIMO schemes, MRT and AS. But, differently from chapter 2, here we also employ multiple antennas at the receiver. Therefore, AS selects a single pair of antennas, one at the transmitter and one at the receiver, while our MRT scheme extends that of (PARK; HEATH, 2016) to the case of a fully MIMO communication.

Therefore, following the Slivnyak's theorem (HAENGGI, 2012), we focus on the typical receiver located at the origin, so that all other transmitters lie at a distance of d_i, $i \in \mathbb{N}$, from the origin. Thus, i denotes each D2D pair, from Tx_i to Rx_i, whose channel matrix is represented by $\mathbf{H}_i \in \mathbb{C}^{N\times N}$. Moreover, without loss of generality, we represent the main link by $i = 1$, and the interference channels due to neighbor devices communicating at the same time are represented by $\mathbf{G}_i \in \mathbb{C}^{N\times N}$.

Thus, the area sum spectral efficiency in such D2D scenario is given by (PARK; HEATH, 2016)

$$\xi_{\text{sch}} = \rho\, A\, \mathcal{R}_{\text{sch}}, \tag{20}$$

expressed in bps/Hz, where $\mathcal{R}_{\text{sch}}$ denotes the spectral efficiency of each employed MIMO scheme, with $\text{sch} \in \{\text{MRT}, \text{AS}\}$.

In addition, the area energy efficiency is defined as

$$\eta_{\text{sch}} = \frac{\xi_{\text{sch}}}{\mathcal{P}_{\text{sch}}}, \tag{21}$$

where $\mathcal{P}_{\text{sch}}$ is the power consumed to transmit one bit of information, while employing

Figure 15 – D2D communication network with devices located within an area A following a PPP distribution. The index i denotes each D2D link, between Tx_i and Rx_i, whose channel matrix is represented by $\mathbf{H}_i \in \mathbb{C}^{N\times N}$. Moreover, the main link is denoted by $i = 1$ and the interference channels due to neighbor devices communicating at the same time are represented by $\mathbf{G}_i \in \mathbb{C}^{N\times N}$.

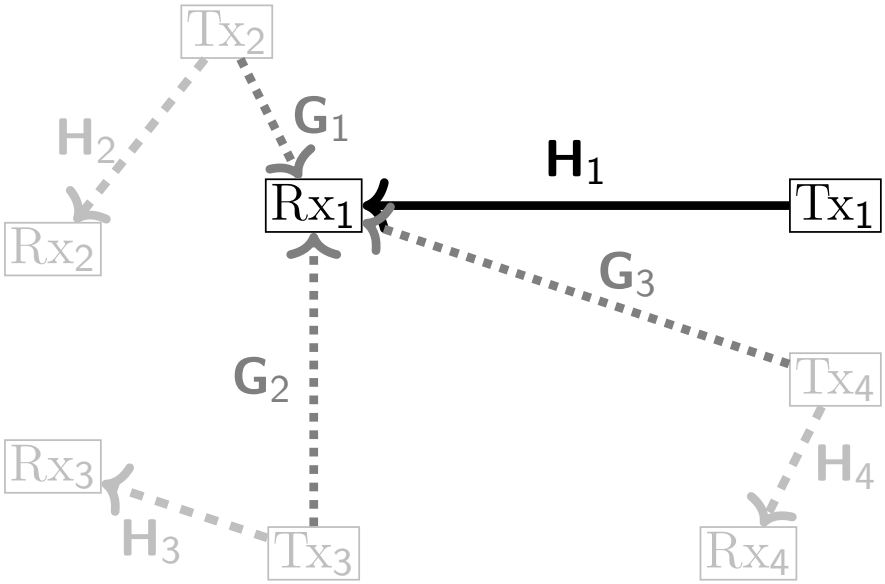

Source: The author

sch as the MIMO transmission scheme, which we define according to (CUI et al., 2005) and (ROSAS et al., 2016) as

$$\mathcal{P}_{\mathrm{sch}} = \frac{P_{\mathrm{t}}}{\psi} + \hat{N}\,(P_{\mathrm{ctx}} + P_{\mathrm{crx}})\,, \tag{22}$$

where P_{t} is the transmit power, ψ is the drain efficiency of the power amplifier, $\hat{N}$ it the number of *active* antennas at each side, which depends on the employed MIMO scheme, while P_{ctx} and P_{crx} represent the power used by the RF circuitry at the transmitter and at the receiver, respectively.

3.2 MIMO TRANSMISSION SCHEMES

3.2.1 Antenna Selection (AS)

Aiming at improved energy efficiency, we employ an AS scheme so that only $\hat{N} = 1$ antenna remains active at each side. Thus, the signal at the receiver Rx_1 is given by

$$y_1 = d_1^{-\alpha/2}\, h_1\, s_1 + \sum_{i=2}^{\infty} d_i^{-\alpha/2}\, g_i\, s_i + w_1, \tag{23}$$

where d_i is the distance between Tx_i and Rx_i, $\forall i$, $h_1 = \max(\|\mathbf{H}_1\|)$ is the channel fading coefficient due the AS, which yields the highest SNR, and g_i represents the interference of the neighbor nodes communicating at the same time. Moreover, $\alpha > 2$ is the path-loss exponent, the average transmitted power is $P_\text{t} = \mathbf{E}[|s_k|^2]$, w_1 is additive white Gaussian noise, with zero-mean and variance σ^2. Thus, the average SNR at the receiver Rx_1 is (PARK; HEATH, 2016; GOLDSMITH, 2005)

$$\overline{\gamma} = \frac{P_\text{t} G \lambda^2}{(4\pi)^2 N_0 W}, \tag{24}$$

where f is the carrier frequency, c is the speed of light in vacuum, G is the antenna gain and W is the bandwidth.

In addition, a feedback channel is required in order to inform the index of the selected antenna to the transmitter, based on the highest instantaneous SNR at the receiver (RAYEL et al., 2014). Thus, the required number of feedback bits (B_sch) is

$$B_\text{AS} = \lceil \log_2(N) \rceil. \tag{25}$$

Then, the signal-to-interference plus noise ratio (SINR) at the receiver obtained from (23) is

$$\epsilon_\text{AS} = \frac{d_1^{-\alpha} h_1^2}{\sum_{i=2}^{\infty} d_i^{-\alpha} g_i^2 + \frac{1}{\overline{\gamma}}}, \tag{26}$$

where we assume that all interfering nodes employ the same transmit power P_t. Moreover, the spectral efficiency ($\mathcal{R}_\text{sch}$) of the AS scheme is given by

$$\mathcal{R}_\text{AS} = \mathbb{E}[\log_2(1 + \epsilon_\text{AS})]. \tag{27}$$

Due to the complexity of (26), we resort to (HAMDI, 2010, Lemma 1) in order to simplify the evaluation of the spectral efficiency given by (27), reproduced here as follows

$$\begin{aligned} \mathbb{E}\left[\ln\left(1 + \frac{\sum_{n=1}^{N} X_n}{\sum_{m=1}^{M} Y_m + a}\right)\right] = \int_0^\infty \frac{\exp(-za)}{z} \left\{1 - \mathbb{E}\left[\exp\left(-z \sum_{n=1}^{N} X_n\right)\right]\right\} \\ \times \mathbb{E}\left[\exp\left(-z \sum_{m=1}^{M} Y_m\right)\right] \mathrm{d}z, \end{aligned} \tag{28}$$

where $X_n > 0$ and $Y_m > 0$ are arbitrary non-negative independent random variables and $a > 0$ is a constant.

Therefore, combining (26)-(28) the ergodic spectral efficiency becomes

$$\mathcal{R}_{\mathrm{AS}} = \log_2(e) \int_0^{\infty} \frac{\exp\left(-d_1^{\alpha}\,\overline{\gamma}^{-1}\,z\right)}{z} \cdot (1-\Phi) \cdot \Psi \,\mathrm{d}z, \tag{29}$$

where

$$\Phi = \mathbb{E}\left[\exp\left(-z h_1^2\right)\right] \tag{30}$$

represents the average with respect to the main link signal, and

$$\Psi = \mathbb{E}\left[\exp\left(-z \sum_{i=2}^{\infty} d_1^{\alpha}\, d_i^{-\alpha} g_i^2\right)\right] \tag{31}$$

denotes the average with respect to the interference.

First, in order to solve (30) we employ the probability density function (PDF) of h_1 assuming selection combining (GOLDSMITH, 2005), so that

$$\begin{aligned} \Phi &= \int_0^{\infty} \exp(-x\,z)\; N^2 \left[1-\exp(-x)\right]^{N^2-1} \exp(-x)\,\mathrm{d}x \\ &= \frac{N^2\,\Gamma(1+z)\,\Gamma(N^2)}{\Gamma(1+z+N^2)}, \end{aligned} \tag{32}$$

where $\Gamma(\cdot)$ is the Gamma function.

In the context of the interference in (31), the mathematical expectancy over the exponential of a random variable X can be written using the Laplace transform, given by (HAENGGI, 2012)

$$\mathcal{L}_X(z) = \mathbb{E}\left[\exp(-zX)\right], \quad z \in \mathbb{C}. \tag{33}$$

Therefore,

$$\Psi = \exp\left(\frac{-\lambda\pi d_1^2}{\mathrm{sinc}\left(\frac{2}{\alpha}\right)} z^{2/\alpha}\right). \tag{34}$$

Finally, combining (29), (32) and (34), the spectral efficiency of AS yields

$$\begin{aligned} \mathcal{R}_{\mathrm{AS}} =& \log_2(e) \int_0^{\infty} \frac{\exp\left(-\frac{d_1^{\alpha}}{\overline{\gamma}} z - \frac{\lambda\pi d_1^2}{\mathrm{sinc}(\frac{2}{\alpha})} z^{2/\alpha}\right)}{z} \times \left(1 - \frac{N^2\,\Gamma(1+z)\,\Gamma(N^2)}{\Gamma(1+z+N^2)}\right) \mathrm{d}z \\ \approx& \log_2(e) \sum_{i=1}^{n} w_i \frac{\exp\left(-\frac{\lambda\pi}{\mathrm{sinc}(\frac{2}{\alpha})} \left(\overline{\gamma}\, x_i\right)^{2/\alpha}\right)}{x_i} \times \left(1 - \frac{N^2\,\Gamma(N^2)\,\Gamma(1+d_1^{-\alpha}\overline{\gamma}\, x_i)}{\Gamma(1+N^2+d_1^{-\alpha}\overline{\gamma}\, x_i)}\right), \end{aligned} \tag{35}$$

where the solution follows the Laguerre-Gauss quadrature (ABRAMOWITZ; STEGUN, 1964, 25.4.45), with x_i being the i-th root of the Laguerre polynomial and w_i being a weight (ABRAMOWITZ; STEGUN, 1964, Table 25.9), where the precision increases with n, where in this work we have employed $n = 15$. This closed-form expression is novel

which is an extension of (PARK; HEATH, 2016).

3.2.2 Maximal Ratio Transmission (MRT)

In the MRT scheme, we assume that all antennas are active at both transmitter and receiver, *i.e.*, $\hat{N} = N$, so that the signal vector at the receiver Rx_1 is given by

$$\mathbf{y}_1 = d_1^{-\alpha/2}\,\mathbf{z}_1^{\dagger}\mathbf{H}_1\mathbf{v}_1 s_1 + \sum_{i=2}^{\infty} d_i^{-\alpha/2}\mathbf{z}_1^{\dagger}\mathbf{G}_i\mathbf{v}_i s_i + \mathbf{w}_1, \tag{36}$$

where $\mathbf{y}_1 \in \mathbb{C}^{N\times N}$, $\mathbf{v}_1$ is the beamforming vector used at the transmitter, $\mathbf{z}_1$ is the combining vector employed at the receiver due to the beamforming operation, and $\mathbf{w}_1$ is the AWGN vector, with zero-mean and variance σ^2, so that the average SNR per receive antenna is $\overline{\gamma} = P_{\mathrm{t}}/\sigma^2$. Then, the SINR at the receiver is given by

$$\epsilon_{\mathrm{MRT}} = \frac{d_1^{-\alpha}|\mathbf{z}_1^{\dagger}\mathbf{H}_1\mathbf{v}_1|^2}{\sum_{i=2}^{\infty} d_i^{-\alpha}|\mathbf{z}_1^{\dagger}\mathbf{G}_i\mathbf{v}_i|^2 + \frac{1}{\overline{\gamma}}}. \tag{37}$$

In addition, similarly to the AS scheme, the ergodic spectral efficiency can be written as

$$\mathcal{R}_{\mathrm{MRT}} = \log_2(e)\int_0^{\infty} \frac{\exp\left(-d_1^{\alpha}\,\overline{\gamma}^{-1}\,z\right)}{z}\cdot(1-\Xi)\cdot\Lambda\,\mathrm{d}z, \tag{38}$$

where the expression related to the main link signal is

$$\Xi = \mathbb{E}\left[\exp\left(-z\,|\mathbf{z}_1^{\dagger}\mathbf{H}_1\mathbf{v}_1|^2\right)\right], \tag{39}$$

while the part related to the interference is

$$\Lambda = \mathbb{E}\left[\exp\left(-z\sum_{i=2}^{\infty} d_1^{\alpha}\,d_i^{-\alpha}|\mathbf{z}_1^{\dagger}\mathbf{G}_i\mathbf{v}_i|^2\right)\right]. \tag{40}$$

Then, in order to solve (39) we assume that the channel coefficients from $\mathbf{H}_1$ are estimated by the receiver and quantized using a codebook known by both transmitter and receiver, so that the comparison with AS in terms of bits of feedback is fairer. Nevertheless, due to the complexity of the design of limited feedback MIMO systems, it is usual to focus on the quantization of the channel magnitude or phase only (KHOSHNEVIS; YU, 2011). When the number of feedback bits is fixed, the authors in (KHOSHNEVIS; YU, 2011) have shown that the optimal number of bits for phase quantization should be $(N-1)/2$ times higher than the number of bits for the channel magnitude. As a result, we follow the channel direction information (CDI) scheme from (YOO et al., 2007) in order to quantize

the channel phase $\tilde{\mathbf{H}}_1 = \mathbf{H}_1/\|\mathbf{H}_1\|$, while we assume that the channel magnitude can use as low as a 1-bit quantization scheme as in (BHASHYAM et al., 2002).

The codebook is denoted by $\mathcal{C}=\{\mathbf{v}_1,\cdots,\mathbf{v}_{2^B}\}$, consisting of 2^B elements, where B is the number of bits employed in the quantization. Then, the receiver quantizes the channel phase of each receive antenna to one of the elements in the codebook, *i.e.*, the one with the minimum Euclidean distance. Then, the codebook indexes for the CDI of each receive antenna are fed back to the transmitter using an error-free zero-delay feedback channel. Assuming a 1-bit quantization scheme the channel magnitude (BHASHYAM et al., 2002), the required number of feedback bits is

$$B_{\text{MRT}} = N(B+1). \tag{41}$$

At the transmitter, the matrix $\hat{\mathbf{H}}_1$ is estimated using the codebook $\mathcal{C}$. Then, the cumulative distribution function (CDF) of the quantization error is given by (PARK; HEATH, 2016)

$$F_{\sin^2\theta_1}(x) = \begin{cases} 2^B x^{N-1} & 0 \le x \le \delta \\ 1 & \delta \le x \end{cases} \tag{42}$$

where $\sin^2\theta_1 = 1 - \left\|\mathbf{H}_1^{\dagger}\hat{\mathbf{H}}_1\right\|^2$ and $\delta = 2^{-\frac{B}{N-1}}$.

Therefore, the average with respect to the main link signal in (39) using the Laplace transform from (33) yields

$$\Xi = (1+z)^{-N^2}\,{}_2F_1\left(N-1, N^2; N; \frac{z\,2^{-\frac{B}{N-1}}}{1+z}\right), \tag{43}$$

whose proof is given in Appendix A and where ${}_2F_1(a,b;c;z)$ is the hypergeometric function. Moreover, let us also remark that the result in (43) extends (PARK; HEATH, 2016, Eq. (6)) to the case when N antennas are employed at the receiver.

Furthermore, using the results from Appendix A to write $|\mathbf{z}_1^{\dagger}\mathbf{G}_i\mathbf{v}_i|^2 = \|\mathbf{G}_i\mathbf{v}_i\|^2$, the average with respect to the interference in (40) yields the same result as for the AS scheme. Thus, from equation (40) and equation (31), $\Lambda = \Psi$, which is also the same as (PARK; HEATH, 2016, theorem 1).

Finally, combining the above with the Laguerre-Gauss quadrature using (ABRAMOWITZ; STEGUN, 1964, Table 25.9), the spectral efficiency of the

MRT scheme yields

$$\mathcal{R}_{\mathrm{MRT}} = \log_2(e) \int_0^{\infty} \frac{\exp\left(-\frac{d_1^{\alpha}}{\overline{\gamma}}\, z - \frac{\lambda \pi d_1^2}{\mathrm{sinc}\left(\frac{2}{\alpha}\right)} z^{2/\alpha}\right)}{z} \tag{44}$$

$$\times \left[1 - \frac{1}{(1+z)^{N^2}}\, {}_2F_1\left(N-1, N^2; N; \frac{z\, 2^{-\frac{B}{N-1}}}{1+z}\right)\right] \mathrm{d}z \tag{45}$$

$$\approx \log_2(e) \sum_{i=1}^{n} w_i \frac{\exp\left(-\frac{\lambda\pi}{\mathrm{sinc}\left(\frac{2}{\alpha}\right)} \left(\overline{\gamma}\, x_i\right)^{2/\alpha}\right)}{x_i} \tag{46}$$

$$\times \left[1 - \left(\frac{d_1^{\alpha}}{\overline{\gamma} x_i + d_1^{\alpha}}\right)^{N^2} {}_2F_1\left(N-1, N^2; N; \frac{2^{-\frac{B}{N-1}}}{1 + \frac{d_1^{\alpha}}{\overline{\gamma} x_i}}\right)\right].$$

3.3 NUMERICAL RESULTS AND DISCUSSION

In this section we provide a few numerical results to illustrate our theoretical analysis. The general simulation parameters, unless stated otherwise, are presented in Table 2, where the system setup follows (PARK; HEATH, 2016), while the parameters related to the power consumption follow (ROSAS et al., 2016; CUI et al., 2005).

Table 2 – System Parameters for the D2D network.

Parameter	Description	Value
G	Antenna gain	5 dBi
α	Path-loss exponent	4
f	Carrier frequency	2.5 GHz
W	Bandwidth	10 KHz
ρ	PPP intensity	$0.56 \times 10^{-3}/\pi$ nodes/m^2
A	Covered Area	$\pi 500^2\,\mathrm{m}^2$
ψ	Power Amplifier Efficiency	0.35
P_{ctx}	RF circuitry power consumption at the TX	11.2 mW
P_{crx}	RF circuitry power consumption at the RX	16.6 mW

Source: According to (PARK; HEATH, 2016; CUI et al., 2005; ROSAS et al., 2016)

First, Figure 16 shows the area sum spectral efficiency (ξ_{sch}) as a function of the average number of nodes. The typical distance is $d_1 = 50$ m, $\overline{\gamma} = 60$ dB and we assume $N \in \{2,4\}$ antennas, corresponding to $B \in \{1,2\}$ bits of feedback, respectively, which implies in $B_{\mathrm{AS}} = \{1,2\}$ and $B_{\mathrm{MRT}} = \{4,12\}$ bits. As we observe, the analytical expressions obtained in (35) and (44) agree very well with the Monte Carlos simulations

Figure 16 – Area sum spectral efficiency (ξ) as a function of the average number of nodes in a fixed area A. The typical distance is $d_1 = 50$ m, $\overline{\gamma} = 60$ dB and $N \in \{2, 4\}$ antennas.

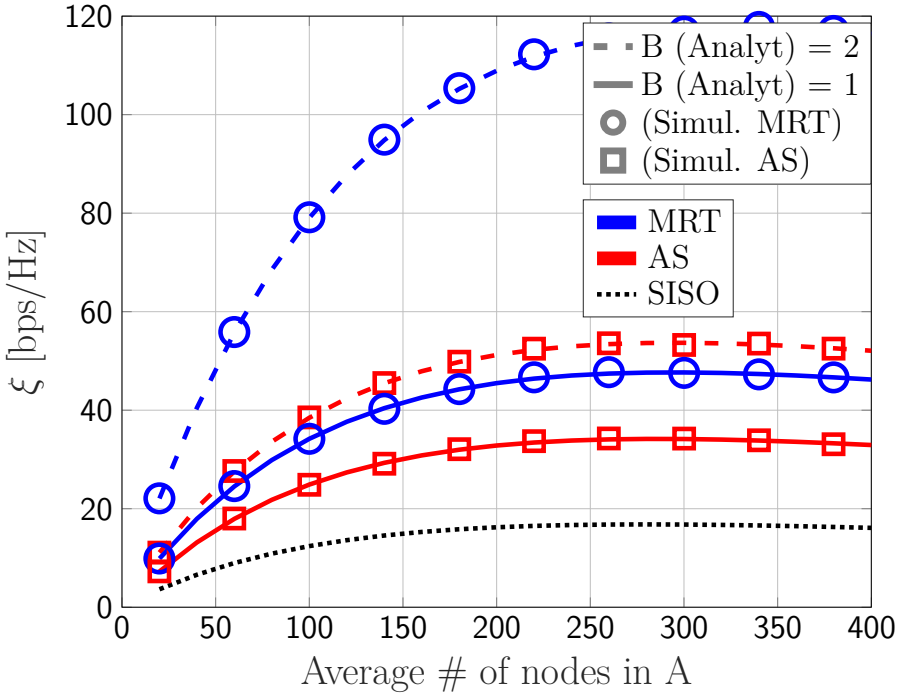

Source: The author

Figure 17 – Area energy efficiency (η) vs. SNR ($\overline{\gamma}$), with $N = 2$ and $B = \{1, \infty\}$.

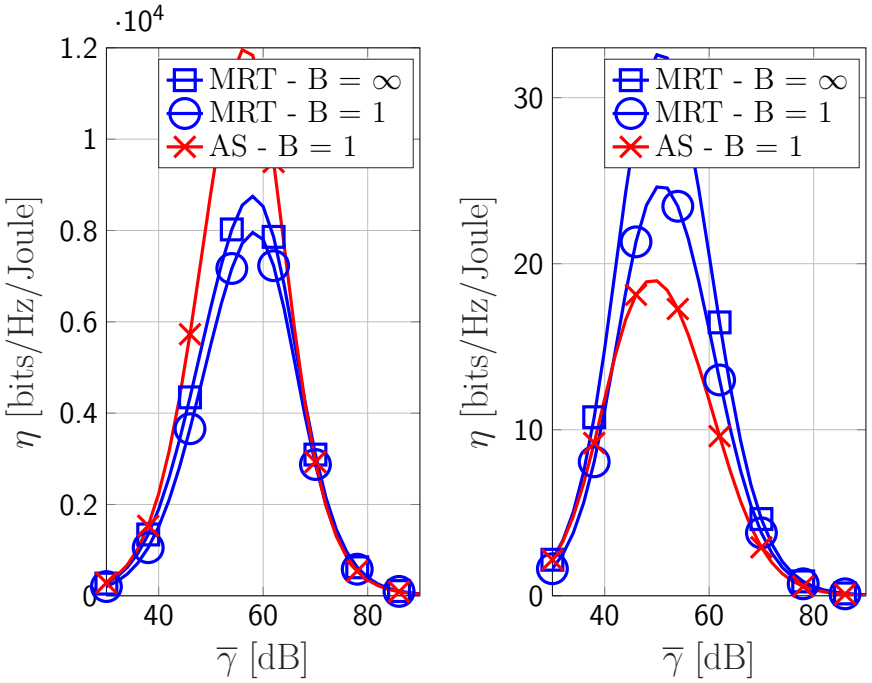

(a) $d_1 = 15$ m (b) $d_1 = 50$ m

for both MIMO schemes. When comparing the curves we observe that both AS and MRT increase ξ_{sch} with respect to SISO, with MRT outperforming AS in terms of spectral efficiency, at the cost of higher total number of feedback bits. This is because in MRT the components of the transmitted signal add coherently, maximizing the SNR at the same time reducing the interference in non intended users. In addition, we can also see that there is an optimal number of nodes that maximize ξ_{sch}, which is higher for MRT than for AS.

Next, Figure 17 plots the area energy efficiency (η_{sch}) as a function of $\overline{\gamma}$, when $d_1 = 15$ m (Figure 17a) and $d_1 = 50$ m (Figure 17b), for $N = 2$ using $B = \{1, \infty\}$ bits of feedback. As we notice, AS has increased area energy efficiency when the devices are closer, outperforming MRT even with $B_{\text{MRT}} = \infty$. However, as d_1 increases, the overall area energy efficiency of both schemes decrease, with MRT performing better than AS. Also, in the same Figure 17, we notice an optimal $\overline{\gamma}$ that maximizes the energy efficiency depends on B, d_1 and on the employed MIMO scheme.

Table 3 shows the distance range in which AS outperforms MRT in terms of area energy efficiency, for the same scenario as in Fig. 17. For instance, with $\overline{\gamma} = 30$ dB AS outperforms MRT up to $d_1 = 161$ m, while the range decreases when $\overline{\gamma}$ increases.

Table 3 – Transmit distance up to which AS outperforms MRT in terms of area energy efficiency, for different $\overline{\gamma}$.

$\overline{\gamma}$	30 dB	40 dB	50 dB	60 dB	70 dB	80 dB
d_1	161 m	91 m	52 m	34 m	24 m	15 m

Finally, Figure 18 complements the analysis for different number of antennas, with B given according to (25). Figure 18a corroborates the results of Figure 17a, once AS has better performance with all antenna arrangements when $d_1 = 5$ m. On the other hand, MRT performs better than AS in Figure 18b, where $d_1 = 25$ m. Nevertheless, Figure 18 indicates that there also exists an optimal number of antennas that maximizes ξ_{sch}, depending on the transmit distance. For instance Figure 18b shows that ξ_{AS} is maximized with $N = 4$ antennas, while and better ξ_{MRT} is maximal with $N = 6$ antennas at a distance of 25 m.

3.4 CONCLUSIONS

In this chapter we compare AS and MRT techniques a D2D network, whose devices share the same spectrum. We have derived spectral efficiency and area energy

Figure 18 – Area energy efficiency η as a function of the number of antennas, with $\overline{\gamma}$= 60 [dB].

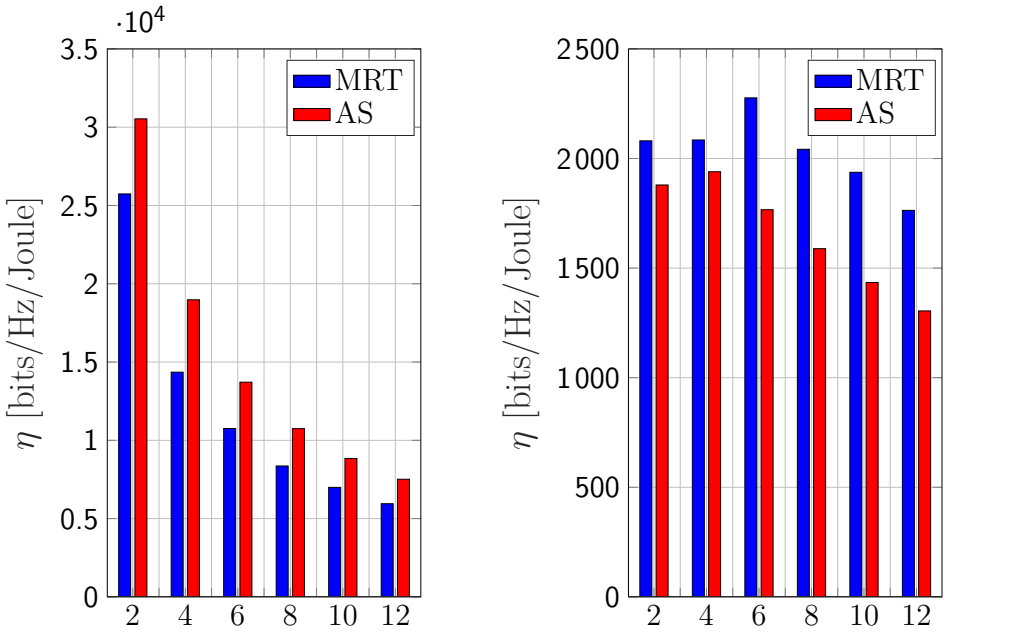

(a) $d_1 = 5$ m (b) $d_1 = 25$ m

Source: The author

efficiency expressions that assume limited feedback, subjected to interference caused by other D2D pairs. In addition, we have modeled the network according to a homogeneous PPP, whose simulations validate the obtained analytical results. Our results show that the MRT scheme always yields better spectral efficiency, even with a very limited number of feedback bits. However, in terms of energy efficiency, AS performs better for short distances, even if BF employs an infinite number of feedback bits.

4 FINAL COMMENTS AND FUTURE EXTENSIONS

Modern network deployments have greater concerns in terms of energy consumption, which encourages the research on energy efficiency in wireless communications. In this work we discuss the energy efficiency based on spatial diversity techniques in two scenarios: first we address the energy savings for the telecommunication provider, employing small base stations; and then we focus on the energy savings reflected in battery savings in a D2D deployment.

In chapter 2 we evaluate a small base station network that employs multiple antenna techniques such as: antenna selection, spatial multiplexing, and maximum ratio transmission. In this context, the goal was to optimize the area energy efficiency by calculating the optimal number of SBSs given some requirements, such as the demanded network capacity, interference and employed MIMO scheme. The results show that when the demand for system capacity is low and the inter-cell interference is not fully canceled, antenna selection emerges with the largest area energy efficiency. On the other hand, if the demanded capacity is higher or if there is a full interference cancellation, spatial multiplexing becomes more energy efficient. Furthermore, we highlight that antenna selection employs more small base stations to achieve the same area throughput as spatial multiplexing. This is an important contribution for a planning engineer considering CAPEX and energy savings. Finally, the performance of the system in terms of area energy efficiency shows to be quite dependent to: i) the amount of interference, which becomes dependent on the interference cancellation scheme; ii) the power consumption model, in the case of the existence of the backhaul, and iii) the amount of energy related to the number of active antennas.

As future extensions for this scenario, user behavior often does not follow a homogeneous traffic model as presented in chapter 2, but rather a model that depends on time and location. Therefore, in order to extend the analysis presented in chapter 2 we could use a traffic distribution where certain areas have a higher demand than others, such as in (GUAN et al., 2013). The mentioned direction could lead us to a mixed optimization, in which certain areas could employ small base stations operating with antenna selection, while other areas may employ spatial multiplexing. In addition, another natural extension is to consider a scenario in which the cells are not hexagonal, but rather modeled by a Poisson distribution, which is a more common approach for 5G networks.

Subsequently, in chapter 3, we evaluate the energy efficiency of a D2D

communication in the presence of other D2D pairs stochastically distributed and interfering with the main link. The nodes employ either antenna selection or maximal ratio transmission. Thus, we show the high dependence of MRT with respect to the number of feedback bits when compared to AS, once fewer feedback bits imply in a very coarse quantization of the CSI, limiting the construction of the beamforming vectors at the transmitter.

In addition, MRT performs better in terms of spectral efficiency than AS, with the advantage increasing when the number of nodes in the network also increases. On the other hand, in terms of energy efficiency, AS has increased performance compared to MRT at short distances, even when the later employs a hypothetically infinite number of feedback bits. Moreover, we also determine the distance for which AS outperforms MRT in terms of energy efficiency as a function of the SNR.

As future extensions of the analysis presented in chapter 3, an interesting analysis is the integration of both D2D and SBS networks as in Figure 19, employing multiple antennas. In this scenario, we could show the impact of the SBS interference over the D2D network, since the transmit power of the SBSs is considerably higher than that employed by the D2D network (MACH et al., 2015).

Figure 19 – Integration of both D2D and SBS networks.

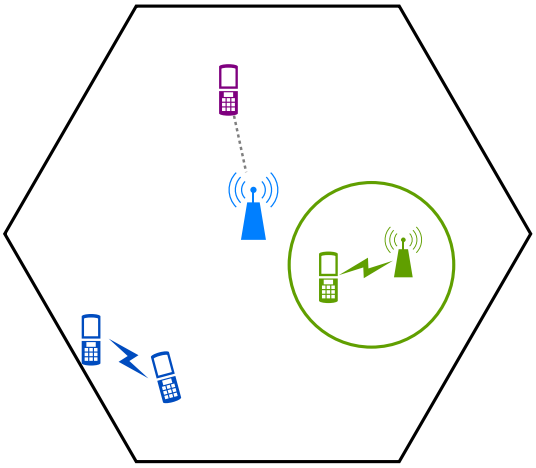

Source: The author

Furthermore, another interesting proposal is to evaluate MIMO-OFDM scenarios, which is a combination of high spectral efficiency over a channel with low multipath distortion and reduced inter symbol interference (STUBER et al., 2004). For instance, the authors in (Zhang; Nabar, 2008; LE et al., 2016) discuss two MIMO-OFDM approaches: bulk and per-subcarrier antenna selection, as shown in Figure 20. The bulk antenna selection chooses a subset of antennas to transmit over all OFDM subcarrier as shown

Figure 20 – MIMO-OFDM antenna selection: (a)Per-subcarrier,(b)Bulk.

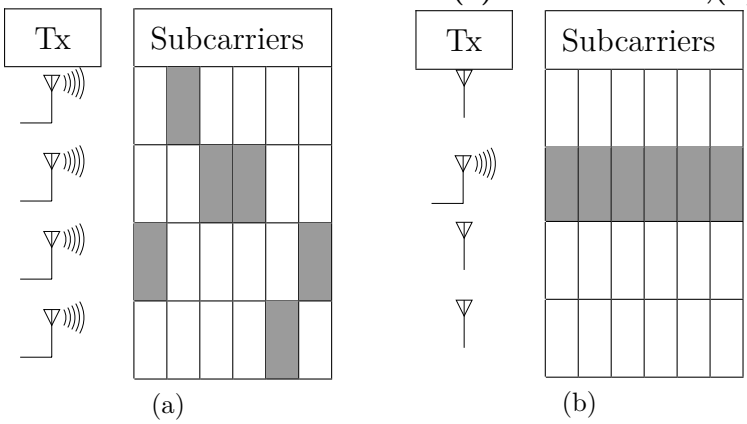

Source: The author

in Figure 20b. In other words, it selects the antennas to maximize the sum-rate of the network. Moreover, per subcarrier antenna selection is made individually for each subcarrier as shown in Figure 20a, which improves robustness reducing the packet error rate (Zhang; Nabar, 2008). It is perceptible that per-subcarrier selection has better capacity than the bulk selection due to its higher degrees of freedom. On in the other hand, the per-subcarrier selection may consume more energy than the bulk selection due to the higher number of RF chains. Then, (LE et al., 2016) proves that bulk selection is more energy efficient than per-subcarrier selection and proposes a greedy algorithm for an adaptive selection method.

Furthermore, in Figure 21 we present our proposal, since neither (LE et al., 2016) nor (Zhang; Nabar, 2008) employed antenna selection at the receiver side, we expect to derive an equation which will represent the antenna selection in the transmitter side over OFDM as in (LE et al., 2016) and contribute with the selection at the receiver side. Moreover, we also aim at the network energy efficiency. Thus, we propose a MIMO-OFDM antenna selection, as shown in Figure 21, which differently from (LE et al., 2016) we also employ antenna selection at the receiver instead of MRC, aiming at higher energy efficiency. Thus, the bulk selection scheme may consume less enery overall, once AS will tend to reduce the interference at the neighbor nodes, consequently improving the energy efficiency.

Finally, another interesting future work is based on the proposal of (PATTANAYAK; KUMAR, 2019) which analyzes the system throughput in a MIMO-OFDM network aiming for an efficient spectrum utilization. Then, the authors propose an algorithm that combines antenna selection and user scheduling, where users employ

Figure 21 – MIMO-OFDM antenna selection extension for Bulk and Per-subcarrier.

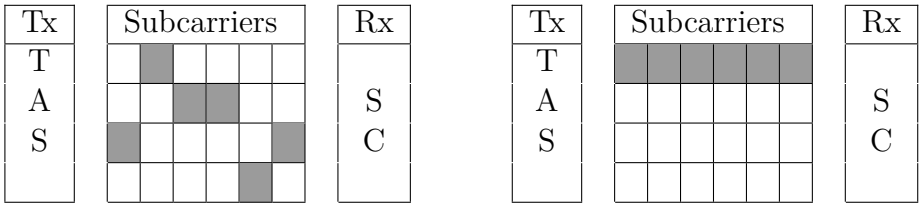

Source: The author

SM with limited feedback. Therefore, the extension of this work to the context of D2D devices, aiming at increased energy efficiency is still open for investigation.

BIBLIOGRAPHY

ABRAMOWITZ, M.; STEGUN, I. **Handbook of Mathematical Functions with Formulas, Graph and Mathematical Tables**. Dover Publications, 1964. ISBN 0-486-61272-4.

ASADI, A.; WANG, Q.; MANCUSO, V. A Survey on Device-to-Device Communication in Cellular Networks. **IEEE Communications Surveys Tutorials**, v. 16, n. 4, p. 1801–1819, Fourthquarter 2014. ISSN 1553-877X.

AUER, G.; GIANNINI, V.; DESSET, C.; GODOR, I.; SKILLERMARK, P.; OLSSON, M.; IMRAN, M. A.; SABELLA, D.; GONZALEZ, M. J.; BLUME, O.; FEHSKE, A. How much energy is needed to run a wireless network? **IEEE Wireless Communication**, v. 18, n. 5, p. 40–49, Oct 2011. ISSN 1536-1284.

AUER, G.; GIANNINI, V.; GODOR, I.; SKILLERMARK, P.; OLSSON, M.; IMRAN, M. A.; SABELLA, D.; GONZALEZ, M. J.; DESSET, C.; BLUME, O. Cellular energy efficiency evaluation framework. In: **Vehicular Technology Conference (VTC Spring)**. 2011. p. 1–6. ISSN 1550-2252.

BHASHYAM, S.; SABHARWAL, A.; AAZHANG, B. Feedback gain in multiple antenna systems. **IEEE Transactions on Communications**, v. 50, n. 5, p. 785–798, May 2002. ISSN 0090-6778.

BJORNSON, E.; SANGUINETTI, L.; HOYDIS, J.; DEBBAH, M. Optimal Design of Energy-Efficient Multi-User MIMO Systems: Is Massive MIMO the Answer? **IEEE Transactions on Wireless Communications**, v. 14, n. 6, p. 3059–3075, Jun. 2015. ISSN 1536-1276.

BOUJELBEN, M.; REJEB, S. B.; TABBANE, S. A comparative study of interference coordination schemes for wireless mobile advanced systems. In: **The 2014 International Symposium on Networks, Computers and Communications**. 2014. p. 1–5.

BRANTE, G.; STUPIA, I.; SOUZA, R. D.; VANDENDORPE, L. Outage Probability and Energy Efficiency of Cooperative MIMO with Antenna Selection. **IEEE Transactions on Wireless Communications**, v. 12, n. 11, p. 5896–5907, November 2013. ISSN 1536-1276.

CHEN, Z.; YUAN, J.; VUCETIC, B. Analysis of Transmit Antenna Selection/Maximal-Ratio Combining in Rayleigh Fading Channels. **IEEE Transactions on Vehicular Technology**, v. 54, n. 4, p. 1312–1321, July 2005. ISSN 0018-9545.

CISCO. **Cisco Visual Networking Index: Forecast and Methodology, 2016 - 2021**. 2017. White Paper.

CISCO. **Cisco Visual Networking Index: Global Mobile Data Traffic Forecast Update, 2017 2022**. fev. 2019. White Paper. Accessed: 2019-10-05.

CUI, S.; GOLDSMITH, A. J.; BAHAI, A. Energy-constrained modulation optimization. **IEEE Transactions on Wireless Communications**, v. 4, n. 5, p. 2349–2360, Sept 2005. ISSN 1536-1276.

DOPPLER, K.; RINNE, M.; WIJTING, C.; RIBEIRO, C. B.; HUGL, K. Device-to-device communication as an underlay to LTE-advanced networks. **IEEE Communications Magazine**, v. 47, n. 12, p. 42–49, Dec 2009. ISSN 0163-6804.

ERICSSON. **Ericsson Mobility Report: On the pulse of the networked society**. jun. 2016. White Paper.

FAHAD, Y. S.; ISOTALO, T.; NIEMELAÄ, J.; VALKAMA, M. Impact of Macrocellular Network Densification on the Capacity, Energy and Cost Efficiency in Dense Urban Environment. **International Journal of Wireless and Mobile Networks**, v. 5, n. 5, p. 99–118, 2013. ISSN 0975-4679.

FENG, D.; JIANG, C.; LIM, G.; CIMINI, L. J.; FENG, G.; LI, G. Y. A survey of energy-efficient wireless communications. **IEEE Communications Surveys Tutorials**, v. 15, n. 1, p. 167–178, First 2013. ISSN 1553-877X.

GOLDSMITH, A. **Wireless Communications**. New York, NY, USA: Cambridge University Press, 2005. ISBN 0521837162.

GUAN, L.; ZHANG, X.; LIU, Z.; HUANG, Y.; LAN, R.; WANG, W. Spatial modeling and analysis of traffic distribution based on real data from current mobile cellular networks. In: **2013 International Conference on Computational Problem-Solving (ICCP)**. 2013. p. 135–138.

HAENGGI, M. **Stochastic Geometry for Wireless Networks**. 1st. ed. New York, NY, USA: Cambridge University Press, 2012. ISBN 1107014697, 9781107014695.

HAENGGI, M.; ANDREWS, J. G.; BACCELLI, F.; DOUSSE, O.; FRANCESCHETTI, M. Stochastic geometry and random graphs for the analysis and design of wireless networks. **IEEE Journal on Selected Areas in Communications**, v. 27, n. 7, p. 1029–1046, September 2009. ISSN 0733-8716.

HAMDI, K. A. A useful lemma for capacity analysis of fading interference channels. **IEEE Transactions on Communications**, v. 58, n. 2, p. 411–416, February 2010. ISSN 0090-6778.

HEI, Y. Q.; ZHANG, C.; SHI, G. M. Trade-off optimization between energy efficiency and spectral efficiency in large scale MIMO systems. **Energy**, v. 145, p. 747 – 753, 2018. ISSN 0360-5442.

HELIOT, F.; IMRAN, M. A.; TAFAZOLLI, R. On the Energy Efficiency-Spectral Efficiency Trade-off over the MIMO Rayleigh Fading Channel. **IEEE Transactions on Communications**, v. 60, n. 5, p. 1345–1356, May 2012. ISSN 0090-6778.

HERNANDEZ-AQUINO, R.; ZAIDI, S. A. R.; MCLERNON, D.; GHOGHO, M. Energy Efficiency Analysis of Two-Tier MIMO Diversity Schemes in Poisson Cellular Networks. **IEEE Transactions on Communications**, v. 63, n. 10, p. 3898–3911, Oct 2015. ISSN 0090-6778.

HU, J.; HENG, W.; LI, X.; WU, J. Energy-Efficient Resource Reuse Scheme for D2D Communications Underlaying Cellular Networks. **IEEE Communications Letters**, v. 21, n. 9, p. 2097–2100, Sept 2017. ISSN 1089-7798.

JIANG, C.; CIMINI, L. J. Antenna Selection for Energy-Efficient MIMO Transmission. **IEEE Wireless Communications Letters**, v. 1, n. 6, p. 577–580, December 2012. ISSN 2162-2337.

KAI, C.; LI, H.; XU, L.; LI, Y.; JIANG, T. Energy-Efficient Device-to-Device Communications for Green Smart Cities. **IEEE Transactions on Industrial Informatics**, v. 14, n. 4, p. 1542–1551, April 2018. ISSN 1551-3203.

KAKITANI, M. T.; BRANTE, G.; SOUZA, R. D.; PELLENZ, M. E.; IMRAN, M. A. Energy and cost analysis of cellular networks under co-channel interference. In: **IEEE Latin-America Conference on Communications**. 2013. p. 1–5. ISSN 2330-989X.

KHAN, M. H. A.; CHUNG, J.-G.; LEE, M. H. Downlink performance of cell edge using cooperative BS for multicell cellular network. **EURASIP J. Wirel. Commun. Netw.**, v. 2016, n. 1, p. 56, 2016. ISSN 1687-1499.

KHOSHNEVIS, B.; YU, W. Bit Allocation Law for Multiantenna Channel Feedback Quantization: Single-User Case. **IEEE Transactions on Signal Processing**, v. 59, n. 5, p. 2270–2283, May 2011. ISSN 1053-587X.

KOUNTOURIS, M.; ANDREWS, J. G. Downlink SDMA with Limited Feedback in Interference-Limited Wireless Networks. **IEEE Transactions on Wireless Communications**, v. 11, n. 8, p. 2730–2741, August 2012. ISSN 1536-1276.

Krauss, R.; Brante, G.; Rayel, O. K.; Souza, R. D.; Onireti, O.; Imran, M. A. Energy efficiency of multiple antenna cellular networks considering a realistic power consumption model. **IEEE Transactions on Green Communications and Networking**, v. 3, n. 1, p. 1–10, March 2019. ISSN 2473-2400.

Krauss, R.; Brante, G.; Souza, R. D.; Onireti, O.; Rayel, O. K.; Imran, M. A. On the area energy efficiency of multiple transmit antenna small base stations. In: **GLOBECOM 2017 - 2017 IEEE Global Communications Conference**. 2017. p. 1–5.

Krauss, R.; Peron, G.; Brante, G.; Souza, R. D. Area energy efficiency of antenna selection in limited feedback device-to-device networks. **IEEE Wireless Communications Letters**, p. 1–1, 2019. ISSN 2162-2337.

LE, N. P.; SAFAEI, F.; TRAN, L. C. Antenna Selection Strategies for MIMO-OFDM Wireless Systems: An Energy Efficiency Perspective. **IEEE Transactions on Vehicular Technology**, v. 65, n. 4, p. 2048–2062, April 2016. ISSN 0018-9545.

LEE, N.; BACCELLI, F.; HEATH, R. W. Spectral Efficiency Scaling Laws in Dense Random Wireless Networks With Multiple Receive Antennas. **IEEE Transactions on Information Theory**, v. 62, n. 3, p. 1344–1359, March 2016. ISSN 0018-9448.

LI, H.; SONG, L.; DEBBAH, M. Energy Efficiency of Large-Scale Multiple Antenna Systems with Transmit Antenna Selection. **IEEE Transactions on Communications**, v. 62, n. 2, p. 638–647, Feb 2014. ISSN 0090-6778.

Lien, S.; Chien, C.; Tseng, F.; Ho, T. 3GPP device-to-device communications for beyond 4G cellular networks. **IEEE Communications Magazine**, v. 54, n. 3, p. 29–35, March 2016.

LIU, L.; CHEN, R.; GEIRHOFER, S.; SAYANA, K.; SHI, Z.; ZHOU, Y. Downlink MIMO in LTE-advanced: SU-MIMO vs. MU-MIMO. **IEEE Communications Magazine**, v. 50, n. 2, p. 140–147, Feb 2012. ISSN 0163-6804.

LOVE, D. J.; HEATH, R. W.; LAU, V. K. N.; GESBERT, D.; RAO, B. D.; ANDREWS, M. An overview of limited feedback in wireless communication systems. **IEEE Journal on Selected Areas in Communications**, v. 26, n. 8, p. 1341–1365, October 2008. ISSN 0733-8716.

LOVE, D. J.; HEATH, R. W.; STROHMER, T. Grassmannian beamforming for multiple-input multiple-output wireless systems. In: **IEEE International Conference on Communications**. 2003. v. 4, p. 2618–2622 vol.4.

MACH, P.; BECVAR, Z.; VANEK, T. In-Band Device-to-Device Communication in OFDMA Cellular Networks: A Survey and Challenges. **IEEE Communications Surveys Tutorials**, v. 17, n. 4, p. 1885–1922, Fourthquarter 2015. ISSN 1553-877X.

MCKAY, M. R.; COLLINGS, I. B.; SMITH, P. J. Capacity and SER analysis of MIMO beamforming with MRC. In: **IEEE International Conference on Communications**. 2006. v. 3, p. 1326–1330. ISSN 1550-3607.

MEHTA, N. B.; KASHYAP, S.; MOLISCH, A. F. Antenna selection in LTE: from motivation to specification. **IEEE Communications Magazine**, v. 50, n. 10, p. 144–150, Oct 2012. ISSN 0163-6804.

MOLISCH, A. F. MIMO systems with antenna selection - an overview. In: **Radio and Wireless Conference (RAWCON)**. 2003. p. 167–170.

NAGATA, S.; XI, W.; YUN, X.; KISHIYAMA, Y.; CHEN, L. Interference measurement scheme for CoMP in LTE-advanced downlink. In: **Vehicular Technology Conference (VTC Spring)**. 2013. p. 1–6. ISSN 1550-2252.

OKUMU, E. M.; DLODLO, M. E. Energy efficient transmit antenna selection for MIMO systems: A cross layer approach. In: **2017 IEEE 7th Annual Computing and Communication Workshop and Conference (CCWC)**. 2017. p. 1–6.

OSMAN, R. A.; PENG, X. H.; TANG, Z. Energy Efficiency and Achievable Data Rate of Device-to-Device Communications in Cellular Networks. In: **IEEE Int. Conf. on Internet of Things (iThings), IEEE Green Computing and Commun. (GreenCom), IEEE Cyber, Physical and Social Computing (CPSCom), and IEEE Smart Data (SmartData)**. 2017. p. 53–59.

PARK, J.; HEATH, R. W. Multiple-Antenna Transmission With Limited Feedback in Device-to-Device Networks. **IEEE Wireless Communications Letters**, IEEE, v. 5, n. 2, p. 200–203, 2016.

PATTANAYAK, P.; KUMAR, P. Combined user and antenna scheduling scheme for MIMO-OFDM networks. **Telecommunication Systems**, v. 70, n. 1, p. 3–12, Jan 2019. ISSN 1572-9451.

RAYEL, O. K.; BRANTE, G.; REBELATTO, J. L.; SOUZA, R. D.; IMRAN, M. A. Energy Efficiency-Spectral Efficiency Trade-Off of Transmit Antenna Selection. **IEEE Transactions on Communications**, v. 62, n. 12, p. 4293–4303, 2014. ISSN 0090-6778.

RENZO, M. D.; HAAS, H.; GHRAYEB, A.; SUGIURA, S.; HANZO, L. Spatial Modulation for Generalized MIMO: Challenges, Opportunities, and Implementation. **Proceedings of the IEEE**, v. 102, n. 1, p. 56–103, Jan 2014. ISSN 0018-9219.

RICHTER, F.; FEHSKE, A. J.; MARSCH, P.; FETTWEIS, G. P. Traffic demand and energy efficiency in heterogeneous cellular mobile radio networks. In: **Vehicular Technology Conference (VTC-Spring)**. 2010. p. 1–6. ISSN 1550-2252.

ROSAS, F.; SOUZA, R. D.; PELLENZ, M. E.; OBERLI, C.; BRANTE, G.; VERHELST, M.; POLLIN, S. Optimizing the Code Rate of Energy-Constrained Wireless Communications With HARQ. **IEEE Trans. on Wireless Commun.**, v. 15, n. 1, p. 191–205, Jan 2016. ISSN 1536-1276.

SAFDAR, G. A.; UR-REHMAN, M.; MUHAMMAD, M.; IMRAN, M. A.; TAFAZOLLI, R. Interference Mitigation in D2D Communication Underlaying LTE-A Network. **IEEE Access**, v. 4, p. 7967–7987, 2016. ISSN 2169-3536.

SHAHAB, A. A. A. S. N.; ZAINUN, A. R. Assessment of Area Energy Efficiency of LTE Macro Base Stations in Different Environments. **Journal of Telecommunications and Information Technology**, n. 1, p. 59–66, 2015.

STUBER, G. L.; BARRY, J. R.; MCLAUGHLIN, S. W.; LI, Y.; INGRAM, M. A.; PRATT, T. G. Broadband mimo-ofdm wireless communications. **Proceedings of the IEEE**, v. 92, n. 2, p. 271–294, Feb 2004. ISSN 0018-9219.

SUN, H.; ZHANG, H.; YANG, T.; LIU, Y. A low complexity scheme for realistic multi-cell downlink coherent joint transmission. In: **2015 IEEE 26th Annual International Symposium on Personal, Indoor, and Mobile Radio Communications (PIMRC)**. 2015. p. 759–763.

TOMBAZ, S.; MONTI, P.; WANG, K.; VASTBERG, A.; FORZATI, M.; ZANDER, J. Impact of Backhauling Power Consumption on the Deployment of Heterogeneous Mobile Networks. In: **IEEE Global Telecommunications Conference - GLOBECOM 2011**. 2011. p. 1–5. ISSN 1930-529X.

TOMBAZ, S.; SUNG, K. W.; ZANDER, J. On Metrics and Models for Energy-Efficient Design of Wireless Access Networks. **IEEE Wireless Communications Letters**, v. 3, n. 6, p. 649–652, Dec 2014. ISSN 2162-2337.

WANG, Z.; VANDENDORPE, L. Antenna Selection for Energy Efficient MISO Systems. **IEEE Communications Letters**, v. 21, n. 12, p. 2758–2761, Dec 2017. ISSN 1089-7798.

XU, S.; ZHANG, H.; TIAN, J.; GUO, S.; ZHOU, X. Distributed energy-efficient resource allocation and power control for device-to-device communications underlaying cellular networks. In: **19th International Symposium on Wireless Personal Multimedia Communications (WPMC)**. 2016. p. 441–446.

YOO, T.; JINDAL, N.; GOLDSMITH, A. Multi-Antenna Downlink Channels with Limited Feedback and User Selection. **IEEE Journal on Selected Areas in Communications**, v. 25, n. 7, p. 1478–1491, September 2007. ISSN 0733-8716.

Zhang, H.; Nabar, R. U. Transmit antenna selection in mimo-ofdm systems: Bulk versus per-tone selection. In: **2008 IEEE International Conference on Communications**. 2008. p. 4371–4375. ISSN 1550-3607.

APPENDIX A – PROOF OF EQUATION (43)

First, let us re-write the term $|\mathbf{z}_1^\dagger \mathbf{H}_1 \mathbf{v}_1|^2$ in (39) using the following inequality (LOVE et al., 2003)

$$|\mathbf{z}_1^\dagger \mathbf{H}_1 \mathbf{v}_1|^2 \leq \|z\|^2 \|\mathbf{H}_1 \mathbf{v}_1\|^2 . \tag{47}$$

Moreover, as in (LOVE et al., 2003) we assume $\|\mathbf{z}_1\|^2 = \|\mathbf{v}_1\|^2 = 1$, which yields $|\mathbf{z}_1^\dagger \mathbf{H}_1 \mathbf{v}_1|^2 = \|\mathbf{H}_1 \mathbf{v}_1\|^2$ and thus

$$\Xi = \mathbb{E}\left[\exp\left(-z\|\mathbf{H}_1 \mathbf{v}_1\|^2\right)\right]. \tag{48}$$

Next, following (PARK; HEATH, 2016; LOVE et al., 2003), and recalling that the receiver employs $\mathbf{v}_1 = \hat{\mathbf{H}}_1$, which is estimated from $\tilde{\mathbf{H}}_1$, we have that

$$\Xi = \mathbb{E}\left[\exp\left(-z\|\mathbf{H}_1\|^2 \left|\tilde{\mathbf{H}}_1^\dagger \hat{\mathbf{H}}_1\right|^2\right)\right] \tag{49}$$

$$= \mathbb{E}\left[\exp\left(-z\|\mathbf{H}_1\|^2 (1-\sin^2\theta_1)\right)\right] \tag{50}$$

$$\overset{(a)}{=} \mathbb{E}_{\sin\theta_1}\left[\left(\frac{1}{1+z\,(1-\sin^2\theta_1)}\right)^{N^2}\right] \tag{51}$$

$$\overset{(b)}{=} \int_0^\delta \left(\frac{1}{1+z\,(1-x)}\right)^{N^2} f_{\sin^2\theta_1}(x)\,\mathrm{d}x, \tag{52}$$

where (a) occurs since $||\mathbf{H}_1||^2$ is a Chi-squared distribution with $2N$ degrees of freedom (CHEN et al., 2005), while $f_{\sin^2\theta_1}(x)$ in (b) is the PDF of the quantization error, obtained as the derivative of (42).

Finally, after some algebraic manipulation, we have that

$$\Xi = 2^B (1+z)^{-N^2} \delta^{N-1}\, {}_2F_1\left(N-1, N^2; N; \frac{z\delta}{1+z}\right), \tag{53}$$

where ${}_2F_1(a,b;c;z)$ is the hypergeometric function. Then, replacing $\delta = 2^{-\frac{B}{N_t-1}}$ we arrive at (43), concluding the proof.